WESTERDIJK FUNGAL BIO DIVERSITY INSTITUTE

Phylogeny of dermatophytes with genomic character evaluation of clinically distinct *Trichophyton rubrum* and *T. violaceum*

P. Zhan[1,2,3,4], K. Dukik[3,4], D. Li[1,5], J. Sun[6], J.B. Stielow[3,8,9], B. Gerrits van den Ende[3], B. Brankovics[3,4], S.B.J. Menken[4], H. Mei[1], W. Bao[7], G. Lv[1], W. Liu[1*], and G.S. de Hoog[3,4,8,9*]

[1]*Institute of Dermatology, Chinese Academy of Medical Sciences & Peking Union Medical College, Jiangsu Key Laboratory of Molecular Biology for Skin Diseases and STIs, Nanjing, China;* [2]*Dermatology Hospital of Jiangxi Provinces, Jiangxi Dermatology Institute, Nanchang, China;* [3]*Westerdijk Fungal Biodiversity Institute, Utrecht, The Netherlands;* [4]*Institute of Biodiversity and Ecosystem Dynamics, University of Amsterdam, Amsterdam, The Netherlands;* [5]*Georgetown University Medical Center, Department of Microbiology and Immunology, Washington, DC, USA;* [6]*Guangdong Provincial Institute of Public Health, Guangdong Provincial Center for Disease Control and Prevention, Guangzhou, China;* [7]*Nanjing General Hospital of Nanjing Command, Nanjing, China;* [8]*Thermo Fisher Scientific, Landsmeer, The Netherlands;* [9]*Center of Expertise in Mycology of Radboudumc/Canisius Wilhelmina Hospital, Nijmegen, The Netherlands*

*Correspondence: W. Liu, liumyco@hotmail.com; G.S. de Hoog, s.hoog@westerdijkinstitute.nl

Abstract: *Trichophyton rubrum* and *T. violaceum* are prevalent agents of human dermatophyte infections, the former being found on glabrous skin and nail, while the latter is confined to the scalp. The two species are phenotypically different but are highly similar phylogenetically. The taxonomy of dermatophytes is currently being reconsidered on the basis of molecular phylogeny. Molecular species definitions do not always coincide with existing concepts which are guided by ecological and clinical principles. In this article, we aim to bring phylogenetic and ecological data together in an attempt to develop new species concepts for anthropophilic dermatophytes. Focus is on the *T. rubrum* complex with analysis of rDNA ITS supplemented with LSU, *TUB2, TEF3* and ribosomal protein L10 gene sequences. In order to explore genomic differences between *T. rubrum* and *T. violaceum*, one representative for both species was whole genome sequenced. Draft sequences were compared with currently available dermatophyte genomes. Potential virulence factors of adhesins and secreted proteases were predicted and compared phylogenetically. General phylogeny showed clear gaps between geophilic species of *Arthroderma*, but multilocus distances between species were often very small in the derived anthropophilic and zoophilic genus *Trichophyton*. Significant genome conservation between *T. rubrum* and *T. violaceum* was observed, with a high similarity at the nucleic acid level of 99.38 % identity. *Trichophyton violaceum* contains more paralogs than *T. rubrum*. About 30 adhesion genes were predicted among dermatophytes. Seventeen adhesins were common between *T. rubrum* and *T. violaceum*, while four were specific for the former and eight for the latter. Phylogenetic analysis of secreted proteases reveals considerable expansion and conservation among the analyzed species. Multilocus phylogeny and genome comparison of *T. rubrum* and *T. violaceum* underlined their close affinity. The possibility that they represent a single species exhibiting different phenotypes due to different localizations on the human body is discussed.

Key words: Adhesion, *Arthrodermataceae*, Character analysis, Dermatophytes, Genome, Phylogeny, Protease, *Trichophyton rubrum*, *Trichophyton violaceum*.

Available online 21 February 2018; https://doi.org/10.1016/j.simyco.2018.02.004.

INTRODUCTION

Dermatophytes (*Onygenales: Arthrodermataceae*) are filamentous fungi that invade and grow in keratin-rich substrates. Many species of this family reside as saprobes in the environment or as commensals in animal fur, but particularly among the anthropophiles there are species that are able to invade hairless human skin and nails and cause infection. About 10 dermatophyte species commonly occur on the human host, and it is estimated that about 20–25 % of the world's population carries a dermatophyte infection (Ates *et al.* 2008; Kim *et al.* 2015). Nearly 80 % of these are caused by *Trichophyton rubrum* and its close relatives (Havlickova *et al.* 2008). The genus *Trichophyton* in the modern sense contains 16 species, of which seven are anthropophilic (de Hoog *et al.* 2017), among which are *T. rubrum* and *T. violaceum*.

Trichophyton rubrum and *T. violaceum* share some significant ecological traits. Both are anthropophilic, i.e. restricted to the human host, causing chronic, non- or mild-inflammatory infections. Their high degree of molecular similarity is expressed in widely used barcoding genes, e.g. rDNA Internal Transcribed Spacer (ITS), translation elongation factor 1 and partial β-tubulin (Gräser *et al.* 2000; Rezaei-Matehkolaei *et al.* 2014; Mirhendi *et al.* 2015). However, the species show significant phenotypic and clinical differences. *Trichophyton rubrum* typically presents as fluffy to woolly, pinkish colonies with moderate growth speed, while *T. violaceum* appears as wrinkled, deep purple colonies with slow growth. Microscopically *T. rubrum* has a profusely branched and richly sporulating conidial system with tear-shaped micro- and cigar-shaped macroconidia. In contrast, hyphae of *T. violaceum* are broad, tortuous and distorted, without sporulation and with chlamydospore-like conidia in older cultures. These morphological differences coincide with marked clinical differences. *Trichophyton rubrum* usually causes infections of glabrous skin leading to tinea corporis, tinea pedis, tinea manuum or onychomycosis (Ates *et al.* 2008). *Trichophyton violaceum* usually infects hair and adjacent skin of the scalp, leading to black dot tinea capitis (Farina *et al.* 2015, Gräser *et al.* 2000; Fig. 1).

The molecular basis of the pathogenicity-associated traits among dermatophytes is currently insufficiently understood to explain the striking differences between the clinical predilections of *Trichophyton rubrum* and *T. violaceum* (Gräser *et al.* 2000). In 2011, the first genomes of dermatophyte species became available; 97 % of the 22.5 Mb genome of *Trichophyton benhamiae* and *T. verrucosum* were completed and aligned (Burmester *et al.* 2011). Shortly afterwards five further genomes of important dermatophytes, *T. rubrum*, *T. tonsurans*, *T. equinum*,

Peer review under responsibility of Westerdijk Fungal Biodiversity Institute.

Studies in Mycology

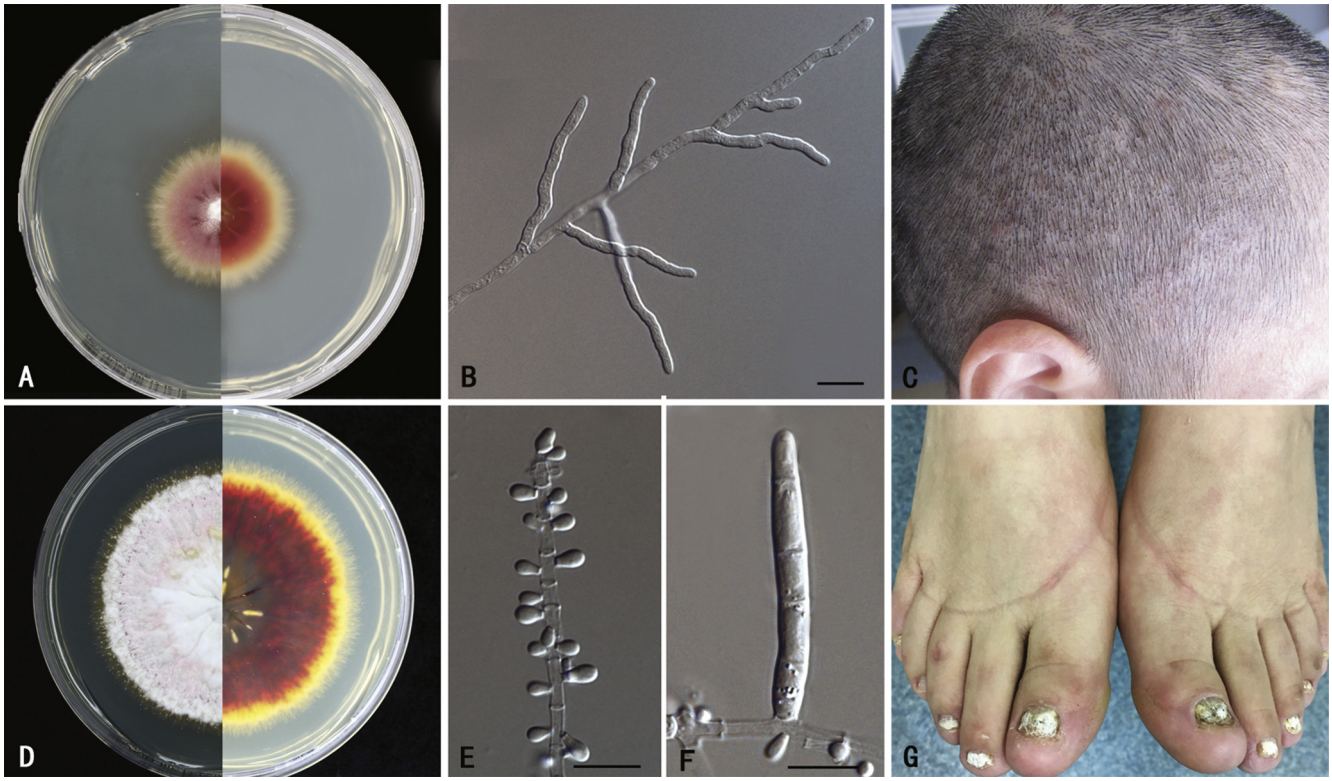

Fig. 1. Phenotypes of two anthropophilic dermatophytes. **A–C.** *Trichophyton violaceum*, CBS 141829. **A.** colony on SGA, 3 wk, 27 °C, obverse and reverse. **B.** non-sporulating hyphae. **C.** clinical image of the isolate (tinea capitis). **D–G.** *Trichophyton rubrum*, CBS 139224. **D.** colony on SGA, 3 wk, 27 °C, obverse and reverse. **E.** microconidia. **F.** macroconidia. **G.** clinical image of the isolate (onychomycosis). Scale bar = 10 µm.

Microsporum canis and *Nannizzia gypsea* were added (Martinez *et al.* 2012). This enabled a comparative analysis of gene families that might be responsible for specific types of pathogenesis, such as proteases, kinases, secondary metabolites and proteins with LysM binding domains. The above species account for the majority of tinea infections; however, the main agent of tinea capitis, *T. violaceum* was not included. To further understand the genetics of *T. rubrum* siblings and their divergent pathomechanisms, we sequenced the genomes of two clinical strains *T. rubrum* CMCC(F)T_{1i} (=CBS 139224) and *T. violaceum* CMCC(F)T_{3l} (=CBS 141829) from South China using Illumina HiSeq®2000 platform. To obtain optimal quality of the reference sequence, PacBio RS single molecule real-time (SMRT) sequencing was also applied to the strain of *T. rubrum*, besides the Illumina methods. Very high genome quality was yielded for both isolates. The draft sequences from our strains were compared with each other and with seven dermatophyte genomes available in the public domain, with a focus on proteases and adhesins. The study allowed us to explore genomic polymorphism in dermatophytes and its implications for pathogenesis and adaptation, aiming to lead to better understanding of genome organization and evolution of specific pathogenic traits.

MATERIALS AND METHODS

Strains and culture conditions

Strains preserved in the reference collection of Centraalbureau voor Schimmelcultures (housed at Westerdijk Fungal Biodiversity Institute) were used to construct a multilocus phylogeny of the family *Arthrodermataceae*. In total, 264 strains were included, of which 261 were from CBS and 3 from BCCM/IHEM Biomedical Fungi and Yeasts Collection, Brussels, Belgium (Table 1). Strains were cultured on Sabouraud's Glucose Agar (SGA) plates inoculated by lyophilized, cryo-preserved or fresh mycelial material. Most of the cultures were grown for 7–14 d at 24 °C. Two strains used for whole-genome sequencing were grown in Sabouraud's glucose broth (SGB); see below.

DNA extraction, PCR, and sequencing

DNA extraction for phylogeny was performed using MasterPure™ Yeast DNA Purification Kit from Epicentre, using preserved material or material harvested from living cultures using methods and PCR protocols of Stielow *et al.* (2015) and de Hoog *et al.* (2017). In total eight gene regions were amplified: ITS and LSU loci of the rDNA operon, partial β-tubulin II (*TUB2*), γ-actin (*ACT*), translation elongation factor 1-α (*TEF1*), RNA polymerase II (*rPB2*), 60S ribosomal protein L10 (*RP 60S L1*) and two primer sets for the fungal-specific translation elongation factor 3 (*TEF3*). The chosen loci, corresponding primer sets, primer sequences, PCR volumes and PCR reactions are given by Stielow *et al.* (2015). After visualization of amplicons on 1 % agarose, positive products were sequenced using ABI big dye terminator v. 3.1, with one quarter of its suggested volume (modified manufacturer's protocol). Bidirectional sequencing was performed using a capillary electrophoresis system (Life Technologies 3730XL DNA analyser). Obtained sequences of CBS strains were manually edited and stored in a BIOLOMICS database at Westerdijk Institute (Vu *et al.* 2012). Consensus sequences of IHEM strains were edited using SeqMan in the LASERGENE 219 software (DNASTAR, WI, U.S.A.).

Alignment, phylogeny and locus assessment

A subset of 123 strains was firstly tested with nine sets of primers for eight DNA loci. In the second analysis, 141 strains were added

Table 1. Strains information in phylogeny study.

CBS number	Current taxon name	New taxon name	Status	Source
CBS 221.75	*A. borellii*	*A. borellii*		Rat
CBS 967.68	*A. borellii*	*A. borellii*	ST *Nannizzia borellii*	Bat
CBS 272.66	*C. georgiae*	*A. ciferrii*	T *Arthroderma ciferrii*	Soil
CBS 492.71	*A. cuniculi*	*A. cuniculi*	ST *Arthroderma cuniculi*	Rabbit burrow
CBS 495.71	*A. cuniculi*	*A. cuniculi*	ST *Arthroderma cuniculi*	Rabbit burrow
CBS 353.66	*A. curreyi*	*A. curreyi*	ET *Arthroderma curreyi*	Soil
CBS 117155	*T. eboreum*	*A. eboreum*	T *Trichophyton eboreum*	Skin
CBS 292.93	*T.* sp.	*A. eboreum*		Skin
CBS 473.78	*A. flavescens*	*A. flavescens*	ST *Arthroderma flavescens*	Kingfisher
CBS 474.78	*A. flavescens*	*A. flavescens*		
CBS 598.66	*A. gertleri*	*A. gertleri*	ST *Trichophyton vanbreuseghemii*	Soil
CBS 666.77	*A. gertleri*	*A. gertleri*		
CBS 228.79	*A. gloriae*	*A. gloriae*	T *Arthroderma gloriae*	Soil
CBS 663.77	*A. gloriae*	*A. gloriae*		
CBS 664.77	*A. gloriae*	*A. gloriae*		
CBS 521.71	*A. insingulare*	*A. insingulare*		Soil
CBS 522.71	*A. insingulare*	*A. insingulare*		Soil
CBS 307.65	*A. lenticulare*	*A. lenticulare*	T *Arthroderma lenticulare*	Gopher burrow
CBS 308.65	*A. lenticulare*	*A. lenticulare*	T *Arthroderma lenticulare*	Gopher burrow
CBS 120.30	*T. tonsurans*	*A. melis*		Human
CBS 669.80	*A. melis*	*A. melis*	T *Arthroderma melis*	Badger burrow
CBS 419.71	*A. multifidum*	*A. multifidum*	ST *Arthroderma multifidum*	Rabbit burrow
CBS 420.71	*A. multifidum*	*A. multifidum*	ST *Arthroderma multifidum*	Rabbit burrow
CBS 132920	*T.* sp.	*A. onychocola*	T *Trichophyton onychocola*	Human
CBS 364.66	*T. phaseoliforme*	*A. phaseoliforme*	ST *Trichophyton phaseoliforme*	Mountain rat
CBS 117.61	*A. quadrifidum*	*A. quadrifidum*	AUT *Arthroderma quadrifidum*	Soil
CBS 118.61	*A. quadrifidum*	*A. quadrifidum*	AUT *Arthroderma quadrifidum*	Soil
CBS 138.26	*A. curreyi*	*A. quadrifidum*		
CBS 310.65	*A. quadrifidum*	*A. quadrifidum*		Soil
CBS 311.65	*A. quadrifidum*	*A. quadrifidum*		Soil
CBS 134551	*T. redellii*	*A. redellii*	T *Trichophyton redellii*	Bat
CBS 132929	*T. thuringiense*	*A. sp.*		Nail
CBS 417.71	*T. thuringiense*	*A. thuringiense*	T *Trichophyton thuringiense*	Mouse
CBS 473.77	*A. tuberculatum*	*A. tuberculatum*	T *Arthroderma tuberculatum*	Blackbird
CBS 101515	*A. uncinatum*	*A. uncinatum*	T *Keratinomyces ajelloi*	Soil
CBS 119779	*T. ajelloi* var. *ajelloi*	*A. uncinatum*		Nail
CBS 128.75	*A. uncinatum*	*A. uncinatum*	ST *E. stockdaleae*	Soil
CBS 179.57	*A. uncinatum*	*A. uncinatum*		Soil
CBS 180.57	*A. uncinatum*	*A. uncinatum*		Soil
CBS 180.64	*A. uncinatum*	*A. uncinatum*	ST *Keratinomyces ajelloi var. nanum*	Soil
CBS 315.65	*A. uncinatum*	*A. uncinatum*	ST *Arthroderma uncinatum*	Soil
CBS 316.65	*A. uncinatum*	*A. uncinatum*	ST *Arthroderma uncinatum*	Soil
CBS 355.93	*C. vespertilii*	*A. vespertilii*	T *Chrysosporium vespertilium*	Bat intestine
CBS 187.61	*Ctenomyces serratus*	*Ctenomyces serratus*	NT *Ctenomyces serratus*	Soil
CBS 544.63	*Ctenomyces serratus*	*Ctenomyces serratus*		Soil
CBS 100148	*A. uncinatum*	*E. floccosum*		Skin
CBS 108.67	*E. floccosum* var. *floccosum*	*E. floccosum*		Human
CBS 230.76	*E. floccosum* var. *floccosum*	*E. floccosum*	NT *Epidermophyton floccosum*	Human

(*continued on next page*)

Table 1. (Continued).

CBS number	Current taxon name	New taxon name	Status	Source
CBS 240.67	*E. floccosum* var. *floccosum*	*E. floccosum*		Skin
CBS 457.65	*E. floccosum* var. *nigricans*	*E. floccosum*		
CBS 553.84	*E. floccosum* var. *floccosum*	*E. floccosum*		Human
CBS 269.89	*Keratinomyces ceretanicus*	*Guarromyces ceretanicus*		
CBS 100083	*A. grubyi*	*L. gallinae*		
CBS 243.66	*A. grubyi*	*L. gallinae*	T *Nannizzia grubyi*	Dog
CBS 244.66	*A. grubyi*	*L. gallinae*		Scalp
CBS 300.52	*A. grubyi*	*L. gallinae*	NT *Lophopyton gallinae*	
CBS 545.93	*M. audouinii*	*M. audouinii*	NT *Microsporum audouinii*	Scalp
CBS 495.86	*A. otae*	*M. audouinii*	T *Nannizzia otae*	
CBS 102894	*M. audouinii*	*M. audouinii*		Scalp
CBS 108932	*M. audouinii*	*M. audouinii*		
CBS 108933	*M. audouinii*	*M. audouinii*		Human
CBS 108934	*M. audouinii*	*M. audouinii*		Human
CBS 119449	*M. audouinii*	*M. audouinii*		Scalp
CBS 404.61	*M. audouinii*	*M. audouinii*	AUT *Sabouraudites langeronii*	Human
CBS 101514	*A. otae*	*M. canis*	T *Microsporum distortum*	Scalp
CBS 114329	*M. canis*	*M. canis*		Skin
CBS 130922	*M. canis*	*M. canis*		Skin
CBS 130931	*M. canis*	*M. canis*		Skin
CBS 130932	*M. canis*	*M. canis*		Skin
CBS 130949	*M. canis*	*M. canis*		Human
CBS 156.69	*A. otae*	*M. canis*		Skin
CBS 191.57	*A. otae*	*M. canis*		Dog
CBS 214.79	*A. otae*	*M. canis*		Rabbit
CBS 217.69	*A. otae*	*M. canis*		Nail
CBS 238.67	*A. otae*	*M. canis*		Human
CBS 274.62	*A. otae*	*M. canis*		Monkey
CBS 281.63	*A. otae*	*M. canis*		Scalp
CBS 283.63	*A. otae*	*M. canis*		
CBS 284.63	*A. otae*	*M. canis*		Gibbon
CBS 445.51	*M. ferrugineum*	*M. canis*		
CBS 482.76	*A. otae*	*M. canis*		Skin
CBS 496.86	*A. otae*	*M. canis*	ST *Nannizzia otae*, NT *Microsporum canis*	Cat
CBS 109478	*M. audouinii*	*M. canis*		Scalp
CBS 317.31	*M. ferrugineum*	*M. ferrugineum*		
CBS 373.71	*M. ferrugineum*	*M. ferrugineum*		Human
CBS 449.61	*M. ferrugineum*	*M. ferrugineum*		
CBS 452.59	*T. concentricum*	*M. ferrugineum*		Skin
CBS 497.48	*M. ferrugineum*	*M. ferrugineum*		Scalp
CBS 366.81	*A. corniculatum*	*N. corniculata*	ST *Nannizzia corniculata*	Soil
CBS 364.81	*A. corniculatum*	*N. corniculata*	ST *Nannizzia corniculata*	Soil
CBS 349.49	*M. duboisii*	*N. duboisii*	T *Sabouraudites duboisii*	Skin
CBS 599.66	*A. fulvum*	*N. fulva*	T *Microsporum boullardii*	Soil
CBS 130934	*M. fulvum*	*N. fulva*		Soil
CBS 130942	*M. fulvum*	*N. fulva*		Human
CBS 146.66	*M. gypseum*	*N. fulva*	AUT *Favomicrosporon pinettii*	Contaminant

Table 1. (Continued).

CBS number	Current taxon name	New taxon name	Status	Source
CBS 147.66	*M. gypseum*	*N. fulva*	AUT *Favomicrosporon pinettii*	Contaminant
CBS 243.64	*A. fulvum*	*N. fulva*	T *Keratinomyces longifusus*	Scalp
CBS 287.55	*A. fulvum*	*N. fulva*	T *Microsporum fulvum*	Human
CBS 385.64	*A. otae*	*N. fulva*		Human
CBS 529.71	*A. fulvum*	*N. fulva*	T *Microsporum ripariae*	Birdnest
CBS 120675	*M. gypseum*	*N. gypsea*		
CBS 100.64	*M. gypseum* var. *vinosum*	*N. gypsea*	ST *Microsporum gypseum var. vinosum*	Skin
CBS 118893	*M. gypseum*	*N. gypsea*		Skin
CBS 130936	*M. gypseum*	*N. gypsea*		Skin
CBS 130939	*M. gypseum*	*N. gypsea*		Skin
CBS 171.64	*A. gypseum*	*N. gypsea*		Soil
CBS 258.61	*A. gypseum*	*N. gypsea*	NT *Gymnoascus gypseus*	Soil
CBS 130948	*M. gypseum*	*N. incurvata*		Skin
CBS 173.64	*A. incurvatum*	*N. incurvata*		Skin
CBS 174.64	*A. incurvatum*	*N. incurvata*	T *Nannizzia incurvata*	Skin
CBS 314.54	*A. obtusum*	*N. nana*	T *Microsporum gypseum var. nanum*	Scalp
CBS 321.61	*A. obtusum*	*N. nana*	ST *Nannizzia obtusa*	Human
CBS 322.61	*A. obtusum*	*N. nana*	ST *Nannizzia obtusa*	Human
CBS 632.82	*A. obtusum*	*N. nana*		Human
CBS 421.74	*A. persicolor*	*N. persicolor*		
CBS 871.70	*A. persicolor*	*N. persicolor*	ST *Nannizzia quinckeana*	Skin
CBS 288.55	*M. praecox*	*N. praecox*	AUT *Microsporum praecox*	Human
CBS 128066	*M. praecox*	*N. praecox*		Skin, from horse
CBS 128067	*M. praecox*	*N. praecox*		Skin, from horse
CBS 121947	*M. amazonicum*	N. sp.		Skin
CBS 450.65	*A. racemosum*	N. sp.	T *Microsporum racemosum*	Rat
CBS 130935	*M. racemosum*	*P. cookei*		Soil
CBS 227.58	*A. cajetanum*	*P. cookei*		
CBS 228.58	*A. cajetanum*	*P. cookei*	T *Microsporum cookei*	Soil
CBS 337.74	*A. cajetanum*	*P. cookei*		Soil
CBS 423.74	*A. racemosum*	*P. cookei*	ST *Nannizzia racemosa*	Soil
CBS 424.74	*A. racemosum*	*P. cookei*	ST *Nannizzia racemosa*	Soil
CBS 101.83	*A. cookiellum*	*P. cookiellum*	ST *Nannizzia cookiella*	Soil
CBS 102.83	*A. cookiellum*	*P. cookiellum*	ST *Nannizzia cookiella*	Soil
CBS 124422	*M. mirabile*	*P. mirabile*	ST *Microsporum mirabile*	Chamois
CBS 129179	*M. mirabile*	*P. mirabile*	ST *Microsporum mirabile*	Nail
CBS 646.73	*A. vanbreuseghemii*	*T. vanbreuseghemii*	T *Arthroderma vanbreuseghemii*	
CBS 809.72	*A. benhamiae*	*T. benhamiae*		
CBS 112368	*A. benhamiae*	*T. benhamiae*		Skin, from guinea pig
CBS 112369	*A. benhamiae*	*T. benhamiae*		Skin, from guinea pig
CBS 112370	*A. benhamiae*	*T. benhamiae*		Skin, from guinea pig
CBS 112371	*A. benhamiae*	*T. benhamiae*		Skin, from guinea pig
CBS 112857	*A. benhamiae*	*T. benhamiae*		Skin, from guinea pig
CBS 112859	*A. benhamiae*	*T. benhamiae*		Skin, from rabbit
CBS 120669	*T. mentagrophytes*	*T. benhamiae*		Guinea pig
CBS 280.83	*A. benhamiae*	*T. benhamiae*		Skin
CBS 623.66	*A. benhamiae*	*T. benhamiae*	ST *Arthroderma benhamiae*	Human

(*continued on next page*)

Table 1. (Continued).

CBS number	Current taxon name	New taxon name	Status	Source
CBS 624.66	*A. benhamiae*	*T. benhamiae*	ST *Arthroderma benhamiae*	
CBS 806.72	*A. benhamiae*	*T. benhamiae*		Guinea pig
CBS 934.73	*A. benhamiae*	*T. benhamiae*		
CBS 131645	*T. bullosum*	*T. bullosum*		Skin
CBS 363.35	*T. bullosum*	*T. bullosum*	T *Trichophyton bullosum*	Horse
CBS 557.50	*T. bullosum*	*T. bullosum*		
CBS 196.26	*T. concentricum*	*T. concentricum*	NT *Trichophyton concentricum*	Skin
CBS 448.61	*T. concentricum*	*T. concentricum*		Skin
CBS 563.83	*T. concentricum*	*T. concentricum*		Skin
CBS 109036	*T. equinum*	*T. equinum*		Skin
CBS 100080	*T. equinum*	*T. equinum*	T *Trichophyton equinum var. autotrophicum*	Horse
CBS 270.66	*T. equinum*	*T. equinum*	NT *Trichophyton equinum*	Horse
CBS 285.30	*T. tonsurans*	*T. equinum*	T *Trichophyton areolatum*	
CBS 634.82	*T. equinum*	*T. equinum*		Horse
CBS 344.79	*T. erinacei*	*T. erinacei*		Skin
CBS 474.76	*T. erinacei*	*T. erinacei*	T *Trichophyton proliferans*	Skin
CBS 511.73	*T. erinacei*	*T. erinacei*	T *Trichophyton mentagrophytes var. erinacei*	Hedghog
CBS 124411	*T.* sp.	*T. erinacei*		Dog
CBS 220.25	*T. eriotrephon*	*T. eriotrephon*	T *Trichophyton eriotrephon*	Skin
CBS 108.91	*T. erinacei*	*T. interdigitale*		
CBS 110.65	*T. mentagrophytes*	*T. interdigitale*		Groin
CBS 113880	*T. mentagrophytes*	*T. interdigitale*		Nail
CBS 117723	*A. vanbreuseghemii*	*T. interdigitale*		Skin
CBS 119447	*T. violaceum*	*T. interdigitale*		Scalp
CBS 232.76	*A. vanbreuseghemii*	*T. interdigitale*		Skin
CBS 425.63	*A. vanbreuseghemii*	*T. interdigitale*	T *Trichophyton batonrougei*	
CBS 428.63	*A. vanbreuseghemii*	*T. interdigitale*	NT *Trichophyton interdigitale*	Skin
CBS 449.74	*A. vanbreuseghemii*	*T. interdigitale*		Skin
CBS 475.93	*A. vanbreuseghemii*	*T. interdigitale*	T *Trichophyton krajdenii*	Skin
CBS 559.66	*A. vanbreuseghemii*	*T. interdigitale*		Skin
CBS 647.73	*A. vanbreuseghemii*	*T. interdigitale*	T *Trichophyton candelabrum*	Nail
CBS 124426	*T. interdigitale*	*T. mentagrophytes*		Dog
CBS 124410	*T. interdigitale*	*T. mentagrophytes*		Dog
CBS 124419	*T. interdigitale*	*T. mentagrophytes*		
CBS 124424	*T. interdigitale*	*T. mentagrophytes*		Chamois
CBS 124425	*T. interdigitale*	*T. mentagrophytes*		Cat
CBS 304.38	*T. radicosum*	*T. mentagrophytes*	T *Trichophyton radicosum*	
IHEM 4268	*T. mentagrophytes*	*T. mentagrophytes*	NT *Trichophyton mentagrophytes*	
CBS 126.34	*T. interdigitale*	*T. mentagrophytes*	T *Bodinia abyssinica*	Skin
CBS 120324	*T. mentagrophytes*	*T. mentagrophytes*		Skin
CBS 120356	*T. mentagrophytes*	*T. mentagrophytes*		Scalp
CBS 124401	*A. benhamiae*	*T. mentagrophytes*		Guinea pig
CBS 124404	*T. interdigitale*	*T. mentagrophytes*		Rabbit
CBS 124408	*T. interdigitale*	*T. mentagrophytes*		Dog
CBS 124415	*T. interdigitale*	*T. mentagrophytes*		Cat
CBS 124421	*T. interdigitale*	*T. mentagrophytes*		Rabbit
CBS 124420	*T. interdigitale*	*T. mentagrophytes*		Rabbit

Table 1. (Continued).

CBS number	Current taxon name	New taxon name	Status	Source
CBS 120357	*T. mentagrophytes*	*T. mentagrophytes*		Scalp
CBS 158.66	*T. mentagrophytes*	*T. quinckeanum*		Skin
CBS 318.56	*T. mentagrophytes*	*T. quinckeanum*	NOT NT *Microsporum mentagrophytes*	Skin
IHEM 13697	*T. quinckeanum*	*T. quinckeanum*	NT *Trichophyton quickeanum*	Mouse
CBS 100081	*T. rubrum*	*T. rubrum*	T *Trichophyton fischeri*	Contaminant
CBS 100084	*T. rubrum*	*T. rubrum*	T *Trichophyton raubitschekii*	Skin
CBS 100238	*T. rubrum*	*T. rubrum*		
CBS 102856	*T. rubrum*	*T. rubrum*		Nail
CBS 110399	*T. rubrum*	*T. rubrum*		Skin
CBS 115314	*T. rubrum*	*T. rubrum*		Nail
CBS 115315	*T. rubrum*	*T. rubrum*		Skin
CBS 115316	*T. rubrum*	*T. rubrum*		Skin
CBS 115317	*T. rubrum*	*T. rubrum*		Human
CBS 115318	*T. rubrum*	*T. rubrum*		Nail
CBS 117539	*T. rubrum* var. *flavum*	*T. rubrum*		Nail
CBS 118892	*T. rubrum*	*T. rubrum*		Nail
CBS 289.86	*T. rubrum*	*T. rubrum*	T *Trichophyton kanei*	Skin
CBS 376.49	*T. rubrum*	*T. rubrum*	T *Trichophyton rodhainii*	Skin
CBS 392.58	*T. rubrum*	*T. rubrum*	NT *Epidermophyton rubrum*	Skin
CBS 592.68	*T. rubrum*	*T. rubrum*	T *Trichophyton fluviomuniense*	Skin
CBS 120425	*T. rubrum*	*T. rubrum*		Nail
CBS 202.88	*T. rubrum*	*T. rubrum*		Skin
CBS 288.86	*T. rubrum*	*T. rubrum*		Contaminant
CBS 118537	*T. schoenleinii*	*T. schoenleinii*		Scalp
CBS 118538	*T. schoenleinii*	*T. schoenleinii*		Scalp
CBS 118539	*T. schoenleinii*	*T. schoenleinii*		Scalp
CBS 433.63	*T. schoenleinii*	*T. schoenleinii*		Scalp
CBS 458.59	*T. schoenleinii*	*T. schoenleinii*	NT *Trichophyton schoenleinii*	Human
CBS 417.65	*A. simii*	*T. simii*		Poultry
CBS 448.65	*A. simii*	*T. simii*	ST *Arthroderma simii*	Poultry
CBS 449.65	*A. simii*	*T. simii*	ST *Arthroderma simii*	Poultry
CBS 520.75	*A. simii*	*T. simii*		Macaca
CBS 109033	*T. tonsurans*	*T. tonsurans*		Horse
CBS 109034	*T. tonsurans*	*T. tonsurans*		Horse
CBS 112186	*T. tonsurans*	*T. tonsurans*		Human
CBS 112187	*T. tonsurans*	*T. tonsurans*		Human
CBS 112188	*T. equinum*	*T. tonsurans*		Horse
CBS 112189	*T. tonsurans*	*T. tonsurans*		Human
CBS 112190	*T. tonsurans*	*T. tonsurans*		Horse
CBS 112191	*T. tonsurans*	*T. tonsurans*		Human
CBS 112192	*T. tonsurans*	*T. tonsurans*		Horse
CBS 112193	*T. equinum*	*T. tonsurans*		Horse
CBS 112194	*T. tonsurans*	*T. tonsurans*		Horse
CBS 112195	*T. tonsurans*	*T. tonsurans*		Horse
CBS 112198	*T. equinum*	*T. tonsurans*		Human
CBS 112856	*A. benhamiae*	*T. tonsurans*		Scalp, zoo transmission

(*continued on next page*)

Table 1. (Continued).

CBS number	Current taxon name	New taxon name	Status	Source
CBS 182.76	*T. tonsurans*	*T. tonsurans*		Horse
CBS 318.31	*T. tonsurans*	*T. tonsurans*	T *Trichophyton floriforme*	
CBS 338.37	*T. immergens*	*T. tonsurans*	T *Trichophyton immergens*	Skin
CBS 496.48	*T. tonsurans*	*T. tonsurans*	NT *Trichophyton tonsurans*	Scalp
CBS 130944	*T. verrucosum*	*T. verrucosum*		Scalp
CBS 130945	*T. verrucosum*	*T. verrucosum*		Skin
CBS 130946	*T. verrucosum*	*T. verrucosum*		Scalp
CBS 130947	*T. verrucosum*	*T. verrucosum*		Skin
CBS 134.66	*T. verrucosum*	*T. verrucosum*		Scalp
CBS 161.66	*T. verrucosum*	*T. verrucosum*		Skin
CBS 282.82	*T. verrucosum*	*T. verrucosum*		Cow
CBS 326.82	*T. verrucosum*	*T. verrucosum*		Cow
CBS 365.53	*T. verrucosum*	*T. verrucosum*	NT *Trichophyton verrucosum*	Cow
CBS 517.63	*T. rubrum*	*T. violaceum*	T *Trichophyton kuryangei*	Scalp
CBS 452.61	*T. violaceum*	*T. violaceum*		Scalp
CBS 118535	*T. violaceum*	*T. violaceum*		Scalp
CBS 119446	*T. violaceum*	*T. violaceum*		Scalp
CBS 120316	*T. violaceum*	*T. violaceum*		Scalp
CBS 120317	*T. violaceum*	*T. violaceum*		Scalp
CBS 120318	*T. violaceum*	*T. violaceum*		Scalp
CBS 120319	*T. violaceum*	*T. violaceum*		Scalp
CBS 120320	*T. violaceum*	*T. violaceum*		Scalp
CBS 178.91	*T.* sp.	*T. violaceum*		Nail
CBS 201.88	*T. violaceum*	*T. violaceum*		Skin
CBS 118548	*M. ferrugineum*	*T. violaceum*		Scalp
CBS 305.60	*T. violaceum*	*T. violaceum*	T *Trichophyton yaoundei*	Scalp
CBS 359.62	*T. balcaneum*	*T. violaceum*	T *Trichophyton balcaneum*	Human
CBS 374.92	*T. violaceum*	*T. violaceum*	NT *Trichophyton violaceum*	Skin
IHEM 19751	*T. soudanense*	*T. violaceum*	NT *Trichophyton soudanense*	Scalp

A = *Arthroderma*; C = *Chrysosporium*; E = *Epidermophyton*; M = *Microsporum*; N = *Nannizzia*; L = *Lophophyton*; P = *Paraphyton*; AUT = authentic; ET = epitype; NT = neotype; ST = syntype; T = (ex-)holotype

for which five chosen loci were analyzed. A phylogenetic tree was constructed using tools provided at http://www.phylogeny.fr/ with and without GBLOCKS to eliminate poorly aligned positions and divergent regions because of the large phylogenetic distance and high divergence of studied taxa. In the *T. rubrum* complex, all known ex-type/ neotype strains of synonymized species were included. In total, 134 strains were successfully amplified.

Obtained sequences were aligned with MAFFT v. 8.850b using default settings, except for the 'genafpair' option (Katoh *et al.* 2009). The nine alignments obtained from the initial dataset of 123 strains were subjected to phylogenetic analysis using maximum likelihood (ML) in MEGA v. 8.0 software. In the second analysis of the total dataset of with 264 strains, RAXML analysis v. 8.0.0 employing GTRCAT model and 1 000 bootstrap replicates and Markov chain Monte Carlo (MCMC) algorithm with MRBAYES v. 3.2.6 in the CIPRES portal (https://www.phylo.org/) were performed.

Multilocus analysis of *T. rubrum* complex

A total of 44 strains were amplified for five genes: ITS with primers ITS4 and ITS5, the D1-D2 region of LSU with primers LR0R and LR5, partial b-tubulin (*TUB2*) with primers TUB2Fd and TUB4Fd, 60S ribosomal protein L10 with 60S-908R and 60-S506F and translation elongation factor 3 (*TEF*3) with primers EF3-3188F and EF3-3984R (Stielow *et al.* 2015). Sequences were aligned with web alignment tool MAFFT. ITS phylogeny tree was reconstructed by MEGA v. 6.06 using Maximum likelihood with Tamura-Nei model and 500 bootstrap replications with *Trichophyton benhamiae* as outgroup. The remaining genes were explored with SNP analysis because of their high degrees of conservation.

Strains and DNA extraction for genome sequencing

Strains used were fresh isolates from cases of onychomycosis (CBS 139224 = CMCC(F)T1$_i$ = *T. rubrum*) and tinea capitis (CBS 141829 = CMCC(F)T3l = *T. violaceum*) of patients in Nanchang, China. Strains were identified as *T. rubrum* and *T. violaceum* on the basis of both phenotypic characters and sequencing (ITS and partial β-tubulin). Cultures were grown in Sabouraud's glucose broth (SGB) incubated at 27 °C for 7–20 d. Cells were harvested

during late log phase by centrifugation at 6 000 *g* for 30 min. Genomic DNA was extracted using the EZNA Fungal DNA kit (Omega Bio-tek, Doraville, GA, USA) according to the manufacturer's instructions. Purified DNA was quantified by TBS-380 fluorometer (Turner BioSystems, Sunnyvale, CA, USA). High quality DNA ($OD_{260/280}$ = 1.8–2.0 > 10 µg) was used for further research.

Library construction and sequencing

For Illumina sequencing, at least 2 µg genomic DNA was used for each strain for library construction. Paired-end libraries with insert sizes of ~300 bp were constructed according to the manufacturer's instructions (AIR™ Paired-End DNA Sequencing Kit, BioScientific, Beijing, China). Sequencing was done using Illumina HiSeq2000 technology with PE100 or PE125 mode. Raw sequencing data was generated by Illumina base calling software CASAVA v. 1.8.2 (http://support.illumina.com/sequencing/sequencing_software/casava.ilmn). Contamination reads, such as ones containing adaptors or primers were identified by SEQPREP (https://github.com/jstjohn/SeqPrep) with parameters: "-q 20 -L 25 -B AGATCGGAAGAGCGTCGTGT-A AGATCGGAAGAGCACACGTC". SICKLE (https://github.com/najoshi/sickle) was applied to conduct reads data trimming with default parameters to get clean data in this study. Clean data obtained by above quality control processes were used to do further analysis.

For PacBio RS (Pacific Biosciences, Menlo Park, CA, USA) sequencing, 8–10 k insert whole genome shotgun libraries were generated and sequenced using standard protocols. An aliquot of 10 µg DNA was spun in a Covaris g-TUBE (Covaris, Woburn, MA, USA) at 3 500 *g* for 60 s using an Eppendorf 5 424 centrifuge (Eppendorf, Hauppauge, NY, U.S.A.). DNA fragments were purified, end-repaired and ligated with SMRTbell™ sequencing adapters following manufacturer's recommendations (Pacific Biosciences). Resulting sequencing libraries were purified three times using 0.45 × vols of Agencourt AMPure XP beads (Beckman Coulter Genomics, Danvers, MA, USA) following the manufacturer's recommendations. PacBio RS sequencing work was performed with C2 reagents.

Genome assembly and annotation

The *T. rubrum* CBS 139224 genome was sequenced using a combination of PacBio RS and Illumina sequencing platforms. The *T. violaceum* CBS 141829 was sequenced by Illumina only. Data were used to evaluate the complexity of the genome and assembled using VELVET (v. 1.2.09) with a k-mer length of 17. Contigs with lengths of less than 200 bp were discarded to increase reliability. The assembly was first produced using a hybrid *de novo* assembly solution modified by Koren *et al.* (2012), in which a de-Bruijn based assembly algorithm and a CLR reads correction algorithm were integrated in a PacBio To CA with CELERA assembler pipeline. The final assembled genome was verified manually.

The protein coding genes (CDS) were predicted with a combination of three gene prediction methods, GENEMARK-ES v. 2.3a (Ter-Hovhannisyan *et al.* 2008), AUGUSTUS v. 2.5.5 (Stanke & Morgenstern 2015) and SNAP (http://korflab.ucdavis.edu/software.html) prediction. The resulting predictions were integrated using GLEAN (Elsik *et al.* 2007).

Open-reading frames with less than 300 base pairs were discarded. The remaining ORFs were queried against non-redundant database (NR in NCBI), SWISSPROT (http://uniprot.org), KEGG (http://www.genome.jp/kegg/), and EGGNOG (http://eggnogdb.embl.de/#/app/home) in view of functional annotation (BLASTX cutoff: e-value < $1e^{-5}$).

Repetitive elements and microsatellites

The assembled genomes of *T. rubrum* CBS 139224 and *T. violaceum* CBS 141829 were searched for repetitive elements by REPBASE (http://www.girinst.org/server/RepBase/index.php) (Bao *et al.* 2015). and REPEATMASKER (http://www.repeatmasker.org/) using the eukaryotic repeat database. A Perl-based script MATFINDER v. 2.0.9 was used for microsatellite identification from assembled scaffolds. The mononucleotide repeats were ignored by modifying the configuration file. The repeat thresholds for di-, tri-, tetra-, penta-, and hexa-nucleotide motifs were set as 8, 5, 5, 5 and 5, respectively. Microsatellite sequences with flanking sequences longer than 50 bp at both sides were collected for future marker development.

Adhesin prediction

Gene families were determined using ORTHOMCL v. 2.0.3 (Inflation value = 1.5, E-value < $1e^{-5}$) and domains were annotated for each orthologous cluster using INTERPROSCAN software (http://www.ebi.ac.uk) with default parameters. On the basis of previous reports of fungal adhesin prediction, six software products were tested, viz. FUNGALRV (Chaudhuri *et al.* 2011), SIGNALP 4.0 (de Groot *et al.* 2013; Teixeira *et al.* 2014), PREDGPIPREDICTOR (http://gpcr2.biocomp.unibo.it/predgpi/pred.htm), FAAPRED (Ramana & Gupta 2010), BIG-PIPREDICTOR (Teixeira *et al.* 2014) and TMHMM (de Groot *et al.* 2013; Teixeira *et al.* 2014). Overall results were evaluated to provide best combinations.

Mitochondrial genome assembly and annotation

The mitochondrial genomes of *T. rubrum* CBS 139224 and *T. violaceum* CBS 141829 were assembled from the Illumina reads using GRAbB (https://github.com/b-brankovics/grabb; Brankovics *et al.* 2016). The mitochondrial genome sequence of *T. rubrum* BMU 01672 (GenBank acc. Nr. FJ385026) was used as a reference for the GRAbB assembly. The final assembly was done using SPADES 3.8.1 (Bankevich *et al.* 2012), which resulted in the assembly of a single circular contig in both cases.

The initial mitochondrial genome annotations were done using MFANNOT (http://megasun.bch.umontreal.ca/) and were manually curated. Annotation of tRNA genes was improved using tRNAscan-SE (Pavesi *et al.* 1994), annotation of intron-exon boundaries was improved by comparing to available reference sequences. Intron encoded proteins were identified using NCBI's ORF FINDER (https://www.ncbi.nlm.nih.gov/orffinder/) and annotated using INTERPRO (Mitchell *et al.* 2015) and CD-SEARCH (Marchler-Bauer & Bryant 2004).

Phylogeny of proteases

Whole genome sequences (nucleotide and amino acid levels) of the nine dermatophytes (*T. rubrum* CBS 118892, *T. tonsurans* CBS

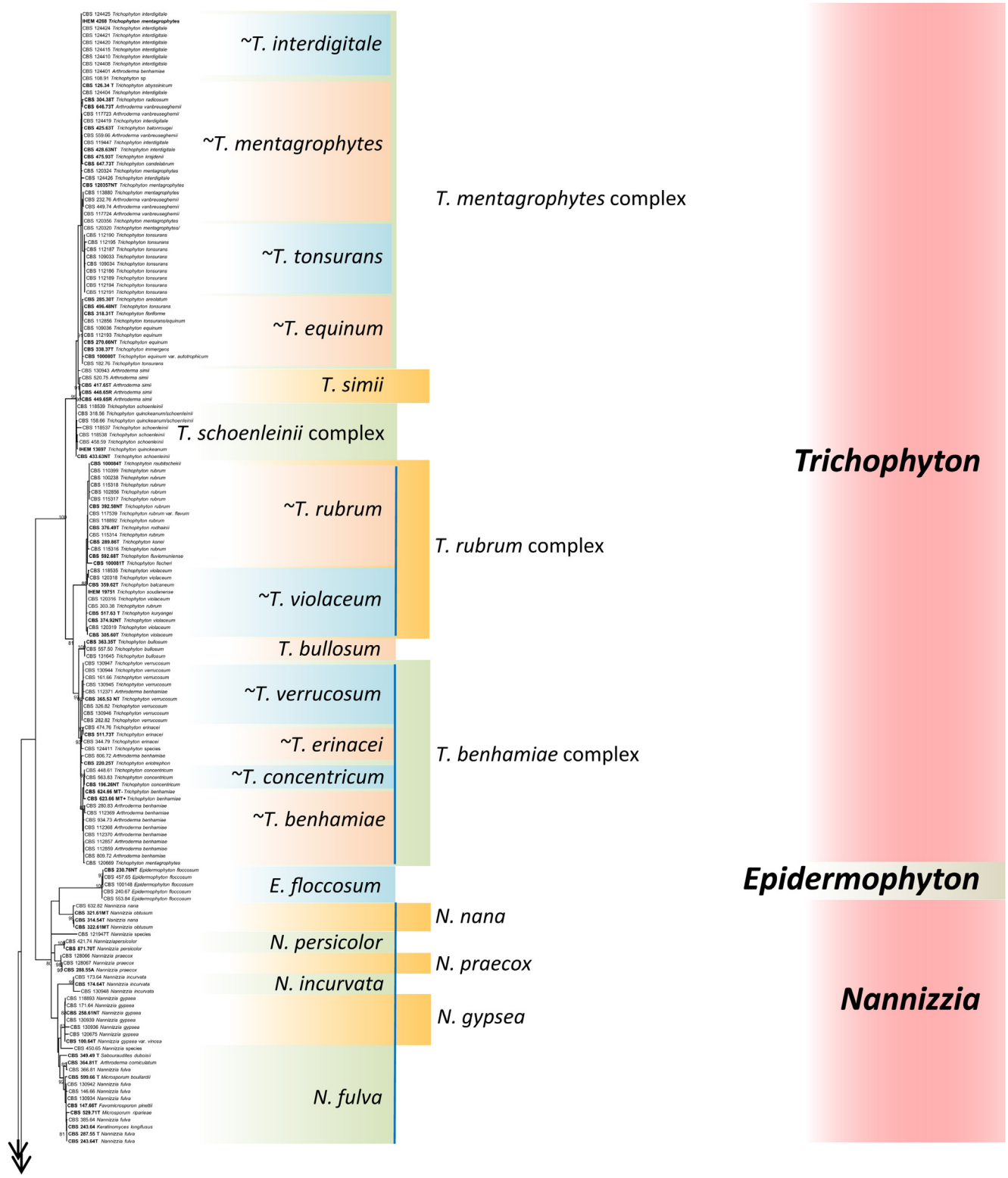

Fig. 2. Maximum likelihood phylogenetic tree of rDNA ITS of 264 dermatophyte strains, using RAXML v. 8.0.0 under GTRCAT model and 1000 bootstrap replications. Bootstrap support above 80 % is shown above branches. Species complexes are indicated when ITS distinction of taxa was not unambiguous (marked with ~). *Guarromyces ceretanicus* CBS 269.89 was used as outgroup. Abbreviations used: A = authentic, ET = epitype, NT = neotype, T = type; MT = mating type. Numbers in bold are authentic or reference for described taxa.

112818, *Nannizzia gypsea* CBS 118893, *Microsporum canis* CBS 113480, *T. equinum* CBS 127.97, *T. benhamiae* CBS 112371, *T. verrucosum* HKI0517) were set as a local database in CLC genomics bench 7.0. Reference protease sequences within the protease families of subtilisins (S8A family), fungalysins (M36 family) and deuterolysins (M35 family) were loaded from UNIPROT database (http://www.uniprot.org/) and homologous sequences were searched in a dermatophyte comparative database (https://olive.broadinstitute.org/projects/Dermatophyte%20Comparative). Orthologs were selected when E-values were less than 10^{-10} and similarities were higher than 90 % at nucleotide level. MEGA v. 6.0 was used to construct the phylogenetic tree. The robustness of the phylogenetic trees calculated by NJ, and the ML approach was estimated by bootstrap analyses with 500 replications using

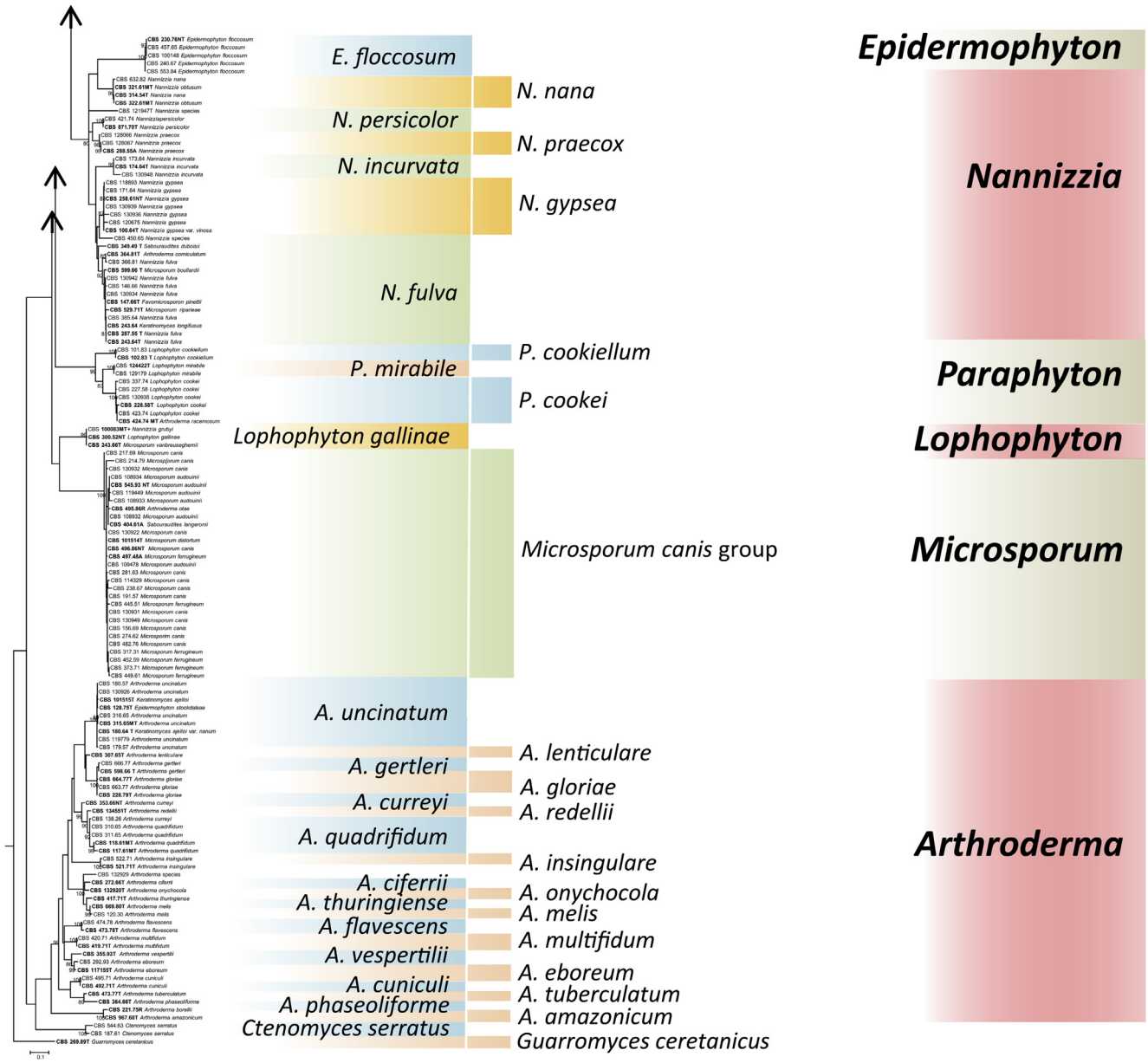

Fig. 2. (Continued).

maximum likelihood and Bayesian techniques. The trees were modified in Adobe Photoshop CS5.

Secondary metabolite biosynthesis

Analysis with the antibiotic and Secondary Metabolite Analysis Shell (antiSMASH; Weber *et al.* 2015) predicted several potential secondary metabolite biosynthesis gene clusters.

RESULTS

ITS phylogeny of dermatophytes

Obtained rDNA ITS sequences were used to construct a taxonomic overview of *Arthrodermataceae* allowing comparison of relative distances between species when ITS is used as barcoding marker. *Guarromyces ceretanicus* was used as outgroup in the tree constructed with Maximum likelihood using RAxML v. 8.0.0 under GTRCAT model and 1000 bootstrap replications (Fig. 2). Bootstrap support above 80 % is shown above branches. In addition to *Guarromyces* and *Ctenomyces*, seven bootstrap-supported clades can be observed which were interpreted by de Hoog *et al.* (2017; Clades A–G) as genera: *Arthroderma, Epidermophyton, Lophophyton. Microsporum, Nannizzia, Paraphyton*, and *Trichophyton*. In this review, *Arthroderma* contains 21 currently accepted species and the ITS tree shows 16 bootstrap-supported branches (76 %); similarly, the multi-species genera *Microsporum* (3 species), *Nannizzia* (9 species), *Paraphyton* (3 species) and *Trichophyton* (16 species) had a ratio of bootstrap-support of 0 %, 56 %, 100 % and 56 %, respectively.

For an assessment of primer sets and resulting phylogenetic trees, we employed four parameters to select loci with superior identification and phylogenetic power and to exclude the ones with poor performance: (1) PCR robustness, (2) number of obtained amplicons, (3) total number of supported clades (BS > 80 %) in trees, and (4) monophyly of the genera. Based on these parameters, *TUB2, RP 60S L1,* and *TEF*3 were chosen for

Table 2. Robustness of phylogenetic trees for ITS LSU, *TUB2, TEF3, RP 60S L1*.

Locus	ITS	LSU	*TUB2*	*TEF3*	RP 60S L1
n = amplicons[1]	238	219	198	211	222
n = clades[2]	40	17	29	17	30

[1] Number of amplicons per locus for the data set of 264 strains.
[2] Number of clades with bootstrap value BS > 70 %, in phylogenetic trees obtained from 147 strains possessing all 5 amplicons.

further analysis along with the standard ITS and LSU loci. From the total set of 264 strains five alignments were created of successfully amplified sequences, containing *n* = 238 (ITS), *n* = 219 (LSU), *n* = 198 (*TUB2*), *n* = 211 (*TEF3*) and *n* = 222 (*RP 60S L1*) sequences respectively (Table 2). The alignments were analyzed using RAXML v. 8.0.0 and MRBAYES v. 3.2.6 analysis with additional RAXML v. 8.0.0 analysis (R147) on the five alignments containing 147 sequences from successfully amplified loci (Table 3). The highest number of supported clades (*n* = 40) was found in ITS three, followed by *RP 60S L1* (*n* = 30), *TUB2* (*n* = 29), and LSU (*n* = 17) and *TEF3* (*n* = 17) (Table 2). Monophyly of seven ITS-defined genera (*Arthroderma, Epidermophyton, Lophophyton, Microsporum, Nannizzia, Paraphyton,* and *Trichophyton*) in *Arthrodermataceae* was taken as lead for attributing clades in the other genes using the three analyses mentioned above are displayed in (Fig. 3). ITS trees were stable, independent from size of data sets or used algorithm. In the largest comparisons, the more remote *Guarromyces ceretanicus* was selected as outgroup because of an unclear position of *Ctenomyces serratus* in these trees, but ITS topology was identical. *Nannizzia* was a supported clade in all three analyses, with lower bootstrap and posterior probability values. In none of the remaining trees, the genus *Nannizzia* was recognized as a monophyletic group. Poor resolution was achieved with *TUB2* and *RP 60S L1,* while LSU and *TEF3* had very poor performance as phylogenetic markers. Since the ITS produced by far the largest number of supported clades, taking another gene as reference would not yield trustworthy results. Therefore, datasets of ITS sequences were concluded to be superior compared to the other four loci, decomposing the entire tree in clades with BS > 80 %. In a final analysis, the *TEF3* dataset was excluded. The tree of concatenated sequences of ITS, *TUB2, RP 60S L1* and partial LSU had similar topology as ITS alone (de Hoog *et al.* 2017).

Polymorphism of *T. rubrum* complex

Polymorphism of the *T. rubrum* complex was explored in 47 strains was analyzed in the *T. rubrum* (*n* = 30) and *T. violaceum* (*n* = 17) (Table S1). LSU, *TUB2, RP 60S L1* and *TEF3* were nearly invariable with only a few SNPs found (data not shown). *TUB2* has two genotypes due to a single difference at position 106 (Fig. S1). In *TEF3* three haplotypes were found, among which 38 (81 %) belonged to a single genotype 1. Four strains (*T. violaceum* CBS 730.88, *T. rubrum* CBS 110399, *T. violaceum* CBS 120319, *T. violaceum* CBS 120318) presented as genotype 2, with six 6 SNPs compared to genotype 1. Five strains (*T. violaceum* CBS 305.60, CBS 374.92, CBS 118535, CBS 120320, CBS 120317) presented as genotype 3 with a single SNP (Fig. S1). In LSU three genotypes were found (Fig. S1). *RP 60S L1* comprised two genotypes, with nine strains of *T. violaceum* deviating from the prevalent type (Fig. S1). ITS showed limited variability (Fig. S2). A group including the neotype CBS 392.58 was nearly monomorphic, with *T. violaceum* separated by four SNPs. A group of strains from various African countries and with *T. rubrum* phenotypes shared characteristics with both main clusters. Strains of the *T. rubrum* cluster had 7 AT repeats at the end of ITS2 while *T. violaceum* mostly had 8–14 and the African *T. rubrum* were variable in this character.

Trichophyton rubrum and *T. violaceum* genomes

For *T. rubrum* CBS 139224, 49.01 M (Pair-End Library) raw reads were generated by Hiseq2000 with PE100 mode. The Q30 value of raw reads was 91.74 % and Q30 of clean data was 95.53 %. In addition, 130473 PacBio subfilter reads (N50 = 2 867 bp) were obtained. A total of 762 contigs (N_{50} = 53 276 bp) were assembled and were joined to create 19 super-scaffolds (scaffold N_{50} of 2 198 313 bp) with the genome size 22.3 Mb. The overall G + C content of entire genome was 48.34 % and the ambiguous bases accounted for 0.055 %. Sequences without Ns that could not be extended at either end were generated to obtain 7 170 unigenes with an average length of 1 677 bp per gene. Coding-gene regions (CDS) accounted for 53.9 % of the genome. Consequently, the intergenic regions were 10 277 739 bp.

In *T. violaceum* CBS 141829, 28.72 M (Pair-End Library) and 21.55 M (Mate-Pair Library) raw reads were generated by Hiseq2000 with PE125 mode. The Q30 value of raw reads was

Table 3. Assessment of phylogenetic trees for ITS, LSU, *TUB2*, *TEF3*, and *RP 60S L1* obtained by Maximum Likelihood in RAxML v8.0.0 and MRBAYES v.3.2.6. Numbers represent bootstrap supports and posterior probabilities of the clades higher than 80% and 0.9 (BS > 80%, PP > 0.9) respectively, representing the genera.

Locus	ITS			LSU			*TUB2*			*TEF3*			*RP 60S L1*		
Software	**B238**	**R147**	**R238**	**B219**	**R147**	**R219**	**B198**	**R147**	**R198**	**B211**	**R147**	**R211**	**B222**	**R147**	**R222**
T	1	100	100	X	X	X	1	99	100	0	0	0	1	98	100
E	1	100	100	1	100	100	1	100	100	1	100	100	1	100	94
N	0.98	85	84	X	X	X	X	X	X	X	X	X	X	X	X
P	1	100	100	0.99	X	86	0.99	0	86	X	X	99	1	100	X
M	1	100	100	1	99	99	1	100	99	1	100	100	1	100	100
A	1	99	95	0	X	83	0.99	95	0	X	X	X	X	0	0
L	1	ND	100	0.97	ND	0	ND	ND	ND	ND	ND	ND	1	ND	100

Abbreviations used: R = RAxML v8.0.0 software; B = MRBAYES v.3.2.6 software; T = *Trichophyton*; E = *Epidermophyton*; N = *Nannizzia*; P = *Paraphyton*; M = *Microsporum*; A = *Arthroderma*; L = *Lophophyton*; ND = no data; X = no clade.

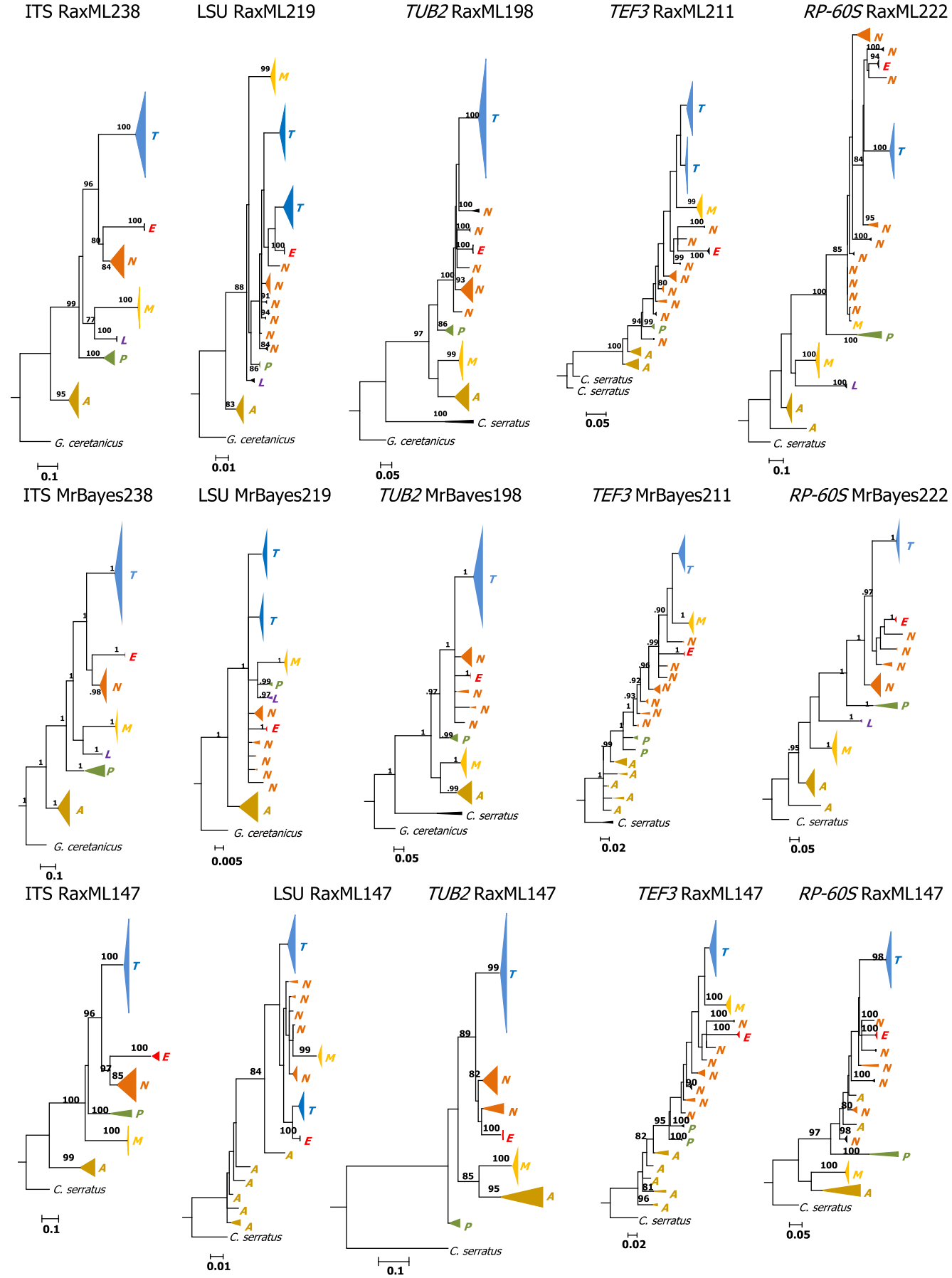

Fig. 3. Comparison of five gene-trees based on maximum datasets of strains analyzed (ITS *n* = 238, LSU *n* = 219, *TUB2* *n* = 198, *TEF3* *n* = 211, *RP-60S L1* *n* = 222), compared with a set of strains for which all genes were sequenced (*n* = 147). Phylogenetic analysis was done with RAXML, MRBAYES, using *Guarromyces ceretanicus* or *Ctenomyces serratus* as outgroup. Bootstrap values > 80 % are shown with the branches.

Table 4. Raw genome data of *T. rubrum* CBS 139224 and CBS 118892, *T. violaceum* CBS 141829.

Index	CBS 139224	CBS 118892	CBS 141829
Isolated sites	China, nail	Germany, nail	China, Scalp
Isolated time	2012	2004	2013
Mating type	*MAT1-1*	*MAT1-1*	*MAT1-1*
Scaffold number	19	36	278
Length of all scaffolds	22 301 977	22 530 013	23 378 626
G + C (%)	48.344 %	48.31 %	47.22 %
Scaffolds N50	2 198 313bp	/	1 335 347bp
No. of genes	7 170	8 804	7 415
N %	0.055 %	/	0.476 %
GC content in gene region (%)	51.2 %	/	51.0 %
Gene/Genome	53.9 %	/	50.6 %
Gene average length	1 677 bp	1 393bp	1 595 bp
Intergenetic region length	10 277 739bp	/	11 549 290 bp
GC content in intergenetic region (%)	44.9 %	/	43.2 %
Intergenetic length/genome (%)	46.1 %	51.69 %	49.4 %

above 90 % and Q30 of clean data was above 93 %. Subsequently 278 scaffolds (N_{50} = 1 335 347 bp) were obtained with a total length of 23 310 379 bp, among of which 77 scaffolds which were longer than 1 000 bp. The G + C content of the genome was 47.22 % with an N-rate of 0.476 %. In total 7 415 genes were predicted with 1,596 bp as average length. Raw data of the two genomes are summarized in Table 4 together with the previously sequenced *T. rubrum* strain CBS 118892.

Comparing *T. rubrum* CBS 139224 *vs.* CBS 118892 (Fig. S2), the latter had a slightly larger genome size (22.5 Mb) with more scaffolds (35) compared to strain CBS 139224 of 22.3 Mb. The genomes were highly similar despite their different geographic origins, but CBS 139224 sequences joined more appropriately with longer scaffolds. At the nucleotide level, the strains revealed a 99.83 % similarity rate. For annotation, the reads were mapped against CBS genome sequences, and combined with *ab initio* gene prediction we annotated 7 170 genes in total in CBS 139224, compared with 7 415 genes in CBS 118892.

Our newly sequenced strains of *T. rubrum vs. T. violaceum* (CBS 139224 and CBS 141829) shared high colinearity at the nucleotide level, with 99.0 % identity (Fig. S3). Eighteen protein coding sequences were annotated, among of which two were specific for CBS 139224 and 16 for CBS 141829 by INTERPRO analysis. The eighteen genes were involved in ATP transferase activity, calcium ion binding and lipid transportation, in addition to four null interpret domains (Table 5). Since they cannot explain the observed differences in pathogenesis, we analyzed the sequence similarity among orthologs of these two strains. In total 6 708 orthologs were obtained, and 85 and 237 paralogs were discovered in CBS 139224 and CBS 141829, respectively. Table 6 lists 14 paralogs with variant duplications. Compared to *T. rubrum* CBS 139224, *T. violaceum* CBS 141829 appeared to have some paralogs with quite different function. For example, A7D00_1963 in *T. rubrum* and A7C99_6543 in *T. violaceum* code for a ribosome biogenesis protein BRX1, while the same ortholog of *T. violaceum* had two additional different domains, coding for a hypothetical protein (A7C99_6542) and an F-box protein

Table 5. Specific domains for *T. rubrum* CBS 139224 and *T. violaceum* CBS 141829 by interpro analysis. "Null"refers to absence of records in Interpro database.

	E-value	ACESSION	IPR-ID	Functional domain	Annotation
T. rubrum CBS 139224	0	A7D00_4483	NULL	NULL	
T. rubrum CBS 139224	0	A7D00_5801	NULL	NULL	
T. violaceum CBS 141829	5.30E-11	A7C99_7410	IPR022414	ATP:guanidophosphotransferase, catalytic domain	transferase activity
T. violaceum CBS 141829	3.70E-18	A7C99_7399	NULL	NULL	
T. violaceum CBS 141829	1.20E-21	A7C99_7396	IPR010009	Apolipophorin-III	lipid transport
T. violaceum CBS 141829	2.20E-11	A7C99_7390	IPR011992	EF-hand domain pair	calcium ion binding
T. violaceum CBS 141829	1.50E-06	A7C99_7408	NULL	NULL	
T. violaceum CBS 141829	4.70E-39	A7C99_7391	IPR022414	ATP:guanidophosphotransferase catalytic domain	transferase activity
T. violaceum CBS 141829	3.10E-20	A7C99_7375	IPR005204	Hemocyanin, N-terminal	
T. violaceum CBS 141829	1.10E-19	A7C99_7415	IPR022413	ATP:guanidophosphotransferase, N-terminal	transferase activity
T. violaceum CBS 141829	5.40E-39	A7C99_7385	IPR000896	Hemocyanin/hexamerin middle domain	
T. violaceum CBS 141829	2.80E-12	A7C99_7394	IPR011992	EF-hand domain pair	calcium ion binding
T. violaceum CBS 141829	1.10E-23	A7C99_7376	IPR005204	Hemocyanin, N-terminal	
T. violaceum CBS 141829	2.90E-102	A7C99_7381	IPR022414	ATP:guanidophosphotransferase, catalytic domain	transferase activity
T. violaceum CBS 141829	1.50E-65	A7C99_7374	IPR005203	Hemocyanin, C-terminal	
T. violaceum CBS 141829	8.20E-11	A7C99_7395	IPR011992	EF-hand domain pair	calcium ion binding
T. violaceum CBS 141829	4.30E-36	A7C99_7404	IPR022413	ATP:guanidophosphotransferase, N-terminal	transferase activity

Table 6. Notable different paralogs of *T. rubrum* CBS 139224 and *T. violaceum* CBS 141829.

	TRCMCC	Probable function	TVCMCC	Probable function
Orthomcl-22	A7D00_722	NIMA-interacting protein TinC	A7C99_4561 A7C99_4562 A7C99_4563 A7C99_4564	NIMA-interacting protein TinC hypothetical protein hypothetical protein hypothetical protein
Orthomcl-33	A7D00_1963	Ribosome biogenesis protein BRX1	A7C99_6542 A7C99_6543 A7C99_6544	hypothetical protein 60S ribosome biogenesis protein Brx1 F-box protein
Orthomcl-37	A7D00_2627	phosphatidylinositol-4- phosphate 5-kinase, PIP5K	A7C99_6653 A7C99_6654 A7C99_6655	hypotheticalprotein CMGC/SRPK protein kinase Serine/threonine-protein kinase SKY1
Orthomcl-39	A7D00_2721	Cell division protein Sep4a	A7C99_523 A7C99_524 A7C99_525	Mitochondrial carrier protein hypothetical protein vacuolar protein sorting-associated protein TDA6
Orthomcl-43	A7D00_2958	dipeptidylaminopeptidase	A7C99_206 A7C99_207 A7C99_208	dipeptidylaminopeptidase succinate dehydrogenase flavoprotein subunit 26S protease regulatory subunit, putative;
Orthomcl-46	A7D00_3180	AAA family ATPase	A7C99_7 A7C99_8 A7C99_9	MFS drug transporter Protein cft1 AAA family ATPase
Orthomcl-50	A7D00_3895	ABC transporter	A7C99_2690 A7C99_2691 A7C99_2692	Aminotransferase ABC transporter hypothetical protein
Orthomcl-53	A7D00_4340	Succinate/fumarate mitochondrial transporter	A7C99_5424 A7C99_5425 A7C99_5426	actin monomer binding protein, putative succinate:fumarateantiporter hypothetical protein
Orthomcl-55	A7D00_4766	Cutinase transcription factor 1 alpha	A7C99_2923 A7C99_2924 A7C99_2925	Killer toxin subunits alpha/beta Cutinase transcription factor 1 alpha hypothetical protein
Orthomcl-57	A7D00_5325	DEAD/DEAH box DNA helicase	A7C99_945 A7C99_946 A7C99_947	hypothetical protein DEAD/DEAH box DNA helicase UDP-galactose transporter
Orthomcl-59	A7D00_7080	phospholipase	A7C99_3575 A7C99_3576 A7C99_3577	Phospholipase hypothetical protein small nuclear ribonucleoprotein
Orthomcl-60	A7D00_814	wd and tetratricopeptide repeat protein	A7C99_4699 A7C99_4700 A7C99_4701	hypothetical protein wd and tetratricopeptide repeat protein hypothetical protein
Orthomcl-4	A7D00_5168 A7D00_5823 A7D00_6142	beta-glucosidase beta-glucosidase beta-glucosidase	A7C99_1137 A7C99_1727 A7C99_1728 A7C99_1729 A7C99_1730 A7C99_1731 A7C99_6784	Probable beta-glucosidase E hypothetical protein beta-1,4-glucosidase 5′-methylthioadenosine phosphorylase Bud site selection protein 22 sugar isomerase beta-glucosidase
Orthomcl-10	A7D00_1852	Vacuolar protein sorting-associated protein 54	A7C99_1678 A7C99_5926 A7C99_5927 A7C99_5928	Vacuolar protein sorting-associated protein 54 hypothetical protein cytochrome P450 Vacuolar protein sorting-associated protein 54

(A7C99_6544). A7D00_2958 encodes a dipeptidylaminopeptidase, while it has two entirely different paralogs in *T. violaceum* (A7C99_207 and A7C99_208). These homologs with diverse evolution maybe related to dermatophyte tissue preference and specialization.

Repetitive sequences and transposable elements

Repetitive sequences (RS) have been shown to serve as vehicle to maintain genomic variability and serves evolutionary change

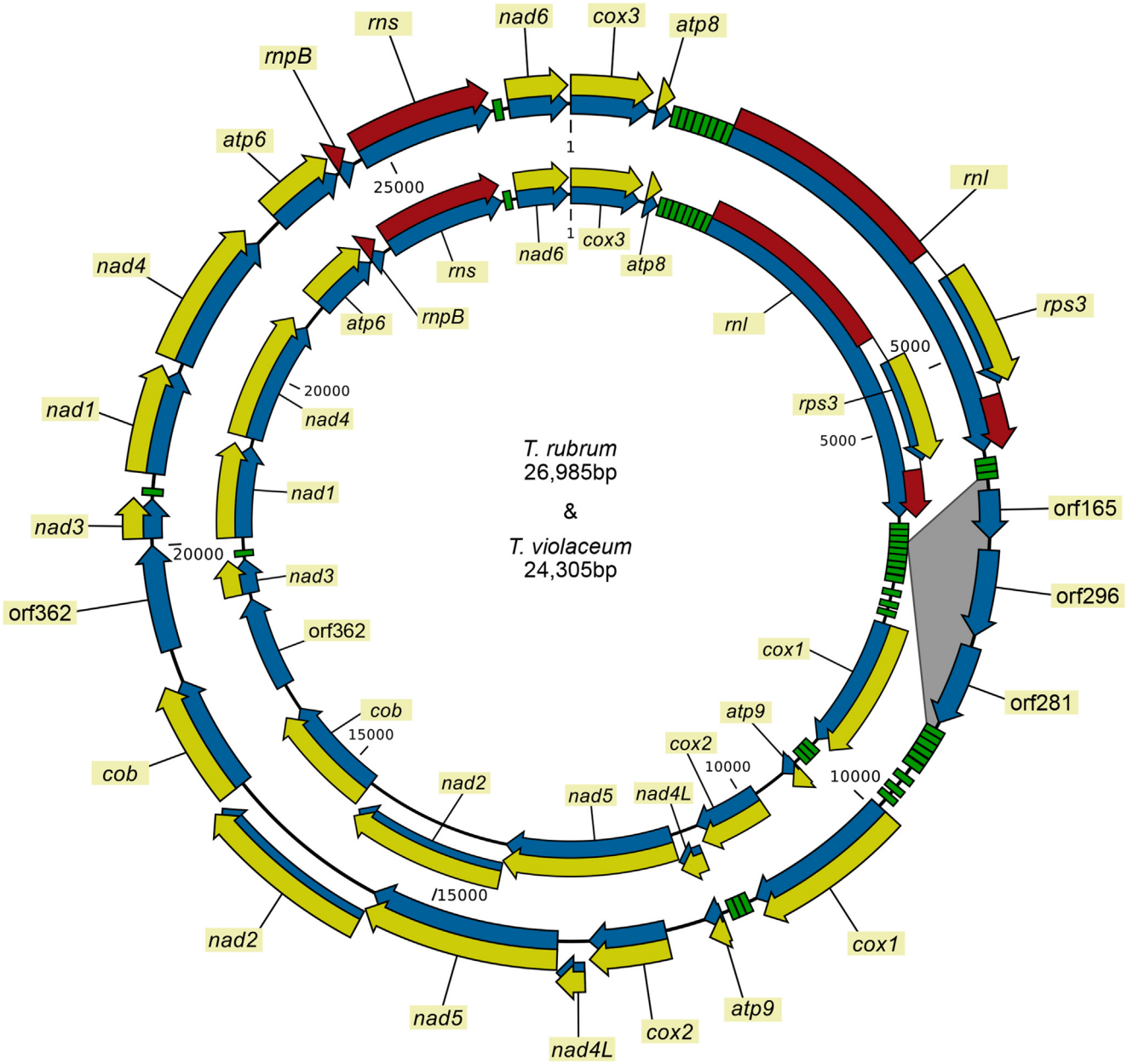

Fig. 4. Mitochondrial genomes of *Trichophyton rubrum* CBS 139224 and *T. violaceum* CBS 141829. Green blocks: tRNA coding genes, blue arrows: genes, yellow arrows: protein coding sequences, red arrows: rDNA coding sequence. ORFs are shown with blue arrows without corresponding yellow arrows.

(Chibana *et al.* 2005). Compared to *Aspergillus* and *Candida*, *T. rubrum* CBS 139224 and *T. violaceum* CBS 141829 have extremely few repeats (Chibana *et al.* 2005, Nierman *et al.* 2005). We identified a total of 77 LRFs (long repeat fragments) in *T. rubrum* occupying 0.04 % of the global genome, and 166 LRFs in *T. violaceum* with a percentage of 0.33 %. The number of transposable elements (TEs) was also low, i.e. 46 in *T. rubrum* (9 209 bp) and 51 in *T. violaceum* (11 354 bp). A total of 92 retrotransposons were predicted within *T. rubrum* with a total length of 10 765 bp and 213 in *T. violaceum* measuring 83 153 bp.

Mitochondria

Mitochondrial genomes were successfully assembled from Illumina reads using GRABB and SPADES. The mitochondrial genomes assembled into single circular contigs for both species (Fig. 4). The lengths of the sequences were 26 985 bp and 24 305 bp for *T. rubrum* CBS 139224 and *T. violaceum* CBS 141829, respectively. The mitochondrial genomes encoded for 13 proteins typical for filamentous fungi, the rRNAs of the small and large subunit of the ribosome (*rns* and *rnl*, respectively) and 25 tRNAs. The *rnl* gene contained a group I intron that codes for *rps3*. Both mitochondrial genomes contain a ribozyme gene, *rnpB*, and an ORF with unknown function between the *cob* and *nad3* genes. The genes in both genomes are in the same orientation and show complete conservation.

The most striking difference between the two mitochondrial genomes is that there is a 2.6 kb insertion in the mitogenome of *T. rubrum* between two tRNA genes that are found downstream the *rnl* gene. The insert is located between *trnV(tav)* and *trnM(cat)*; in *T. violaceum* there is only a single nucleotide separating the two genes, while in *T. rubrum* there is a more than 2.6 kb region separating them. This region contains 3 ORFs, the first of them encodes a putative GIY-YIG endonuclease, the other two have no functional prediction. GIY-YIG endonucleases belong to the homing endonucleases that are frequently found in group I introns.

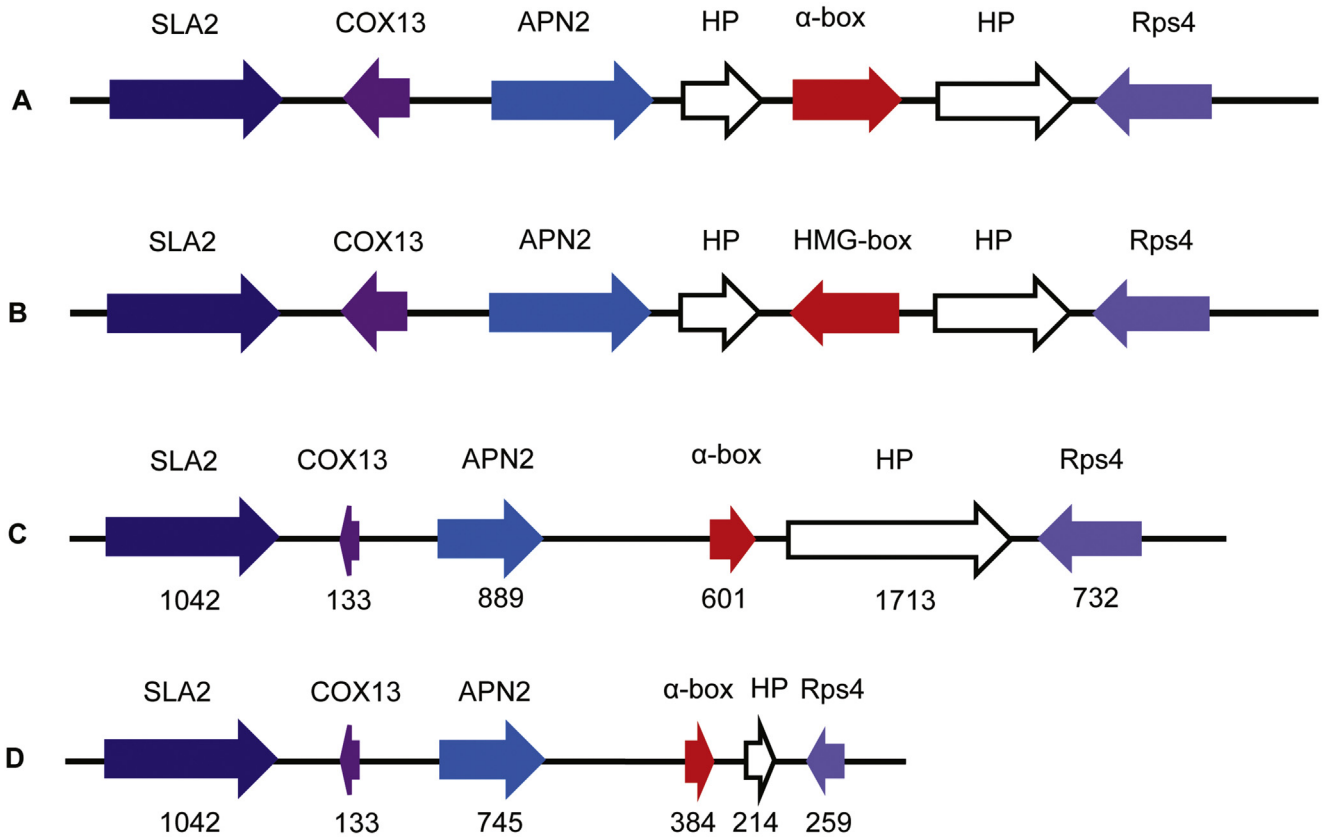

Fig. 5. A, B. Approximate *MAT1-1* locus of dermatophytes. **A.** Locus as present in *T. rubrum* CBS 118892, *T. tonsurans* CBS 112818, *T. verrucosum* HKT0517, *T. benhamiae* CBS 112371, *N. gypsea* CBS 118893, and *M. canis* CBS 113480. **B.** *MAT1-2* locus present in *T. equinum* CBS 127.97. **C, D.** *MAT1-1* locus with numbers of amino acids. **C.** *T. rubrum* CBS 139224. **D.** *T. violaceum* CBS 141829.

Functional classification of EGGNOG

The gene sequences of *T. rubrum* CBS 139224 and *T. violaceum* CBS 141829 were compared against NCBI, SWISS-Prot, KEGG and EGGNOG databases. The prediction of gene function from EGGNOG revealed 3 491 orthologous genes which accounted for 48.8 % of entire genome in *T. rubrum* CBS 139224, while *T. violaceum* CBS 141829, 6 081 orthologs were generated by EGGNOG annotation and took a percentage of 82.01 % of the genome. A comparison of EGGNOG classification of *T. rubrum* CBS 139224 and *T. violaceum* CBS 141829 is provided in Table S2.

Although the total numbers of genes annotated by the database tools are similar, the annotation power seems to be different in each category. In main traits *T. violaceum* and *T. rubrum* histograms were similar, but the former was consistently somewhat higher, which might due to more orthologous genes annotated in *T. violaceum*. Genes involved in cell wall biogenesis [M], cell motility [N] and extracellular structures [W] take small percentages in COG classification, related to the lack of reference databases.

Genes related to metabolism

A total of 2 585 genes involved in 277 metabolic pathways were annotated in *T. rubrum* CBS 139224 according to KEGG functional analysis, while 2 888 genes were predicted for *T. violaceum* CBS 141829 involving in 174 pathways. Table S3 displays the top-14 pathways containing more than 50 genes. Genes of carbohydrate metabolism corresponding to glycosis/gluconeogenesis, TCG cycle, and degradation of pentose phosphate, fructose, mannose, sucrose, and ketone are all present in *T. rubrum* and *T. violaceum*. Key genes responsible for lipid biosynthesis and catabolism were also annotated, including metabolism of triglycerides, glycerophospholipids, and sphingolipids. However, metabolism of arachidonic acid and linoleic acid, and the alpha-linolenic acid pathway were not complete in both fungi analyzed. *Trichophyton rubrum* and *T. violaceum* possess all pathways for biosynthesis and metabolism of the 20 basic amino acids. In addition, arginine succinate lyase, ornithine carbamoyl transferase are also identified and so does a complete urea cycle. Critical genes in porphyrin metabolic pathways are enriched; however, chlorophyll synthesis pathway is interrupted in these two dermatophytes.

Most vitamins, such as thiamine, riboflavin, vitamin B6, nicotinate and icotinamide, pantothenate, and CoA biosynthesis, folate and biotin metabolism were all found in *T. rubrum* and *T. violaceum*, but ascorbate and aldarate metabolism were missing. Both dermatophytes encode the genes that transfer nitrogen residues to L-asparagine, glycine and L-glutamate and break down the latter into ammonia. The sulfur reduction and fixation pathway is also complete in these two strains. *Trichophyton violaceum* has been reported to be vitamin B dependent, growing better and sporulating abundantly in vitamin B-rich media (Gräser *et al.* 2000). Surprisingly, however, the fungus shares this vitamin pathway with *T. rubrum* and shows no deficiency. Overall, the above analysis demonstrates that *T. rubrum* and its molecular siblings possess basic metabolic abilities as most eukaryotic organisms.

Mating type locus

While a sexual life cycle with ascigerous gymnothecia has been described for some zoophilic *Trichophyton* species, mating

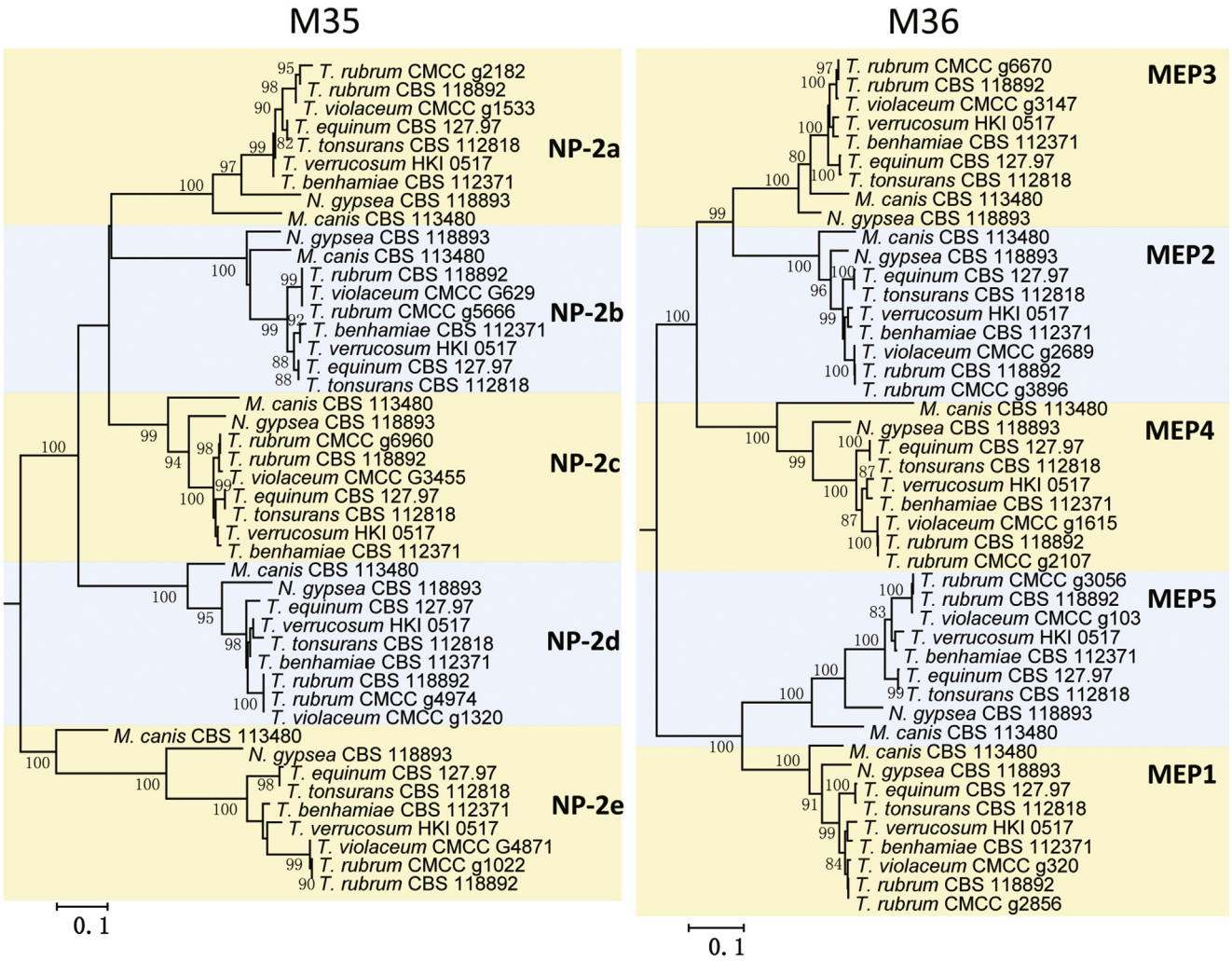

Fig. 6. Non-rooted Maximum likelihood trees of dermatophyte deuterolysins (M35 family) and fungalysins (metalloproteinases, M36 family) constructed with MEGA v. 6.0 with 500 bootstrap replications. *M35 family members denominated herewith.

within *T. rubrum* and *T. violaceum* has not been observed, and it is unclear whether sexuality plays an important role in their natural ecology. Sexual reproduction in heterothallic ascomycetes is governed by a single mating type locus (*MAT*) with two idiomorphs of highly divergent sequences: either alpha (*MAT1-1*) or high mobility group, HMG (*MAT1-2*) (Li *et al.* 2010). *Trichophyton rubrum* CBS 139224 and *T. violaceum* CBS 141829 are identified as of *MAT1-1* type, with upstream *SLA2, COX3* and *APN2* and downstream the 40S rDNA encoding gene as the flanking regions (Fig. 5). With the exception of *T. equinum* CBS 127.97, which is *MAT1-2*, all remaining strains are *MAT1-1* type. The *MAT* region, compared in nine dermatophyte species by local blast in the CLC genomics bench, proved to be highly conserved (Fig. 5). Some variation is noted in the number of amino acids of *MAT* flanking regions of *T. rubrum* and *T. violaceum* (Fig. 5C and D).

Adhesion

Following previous reports, six web servers/platforms with fungal adhesin predictors were consulted to search putative adhesin-like proteins (see Methods). However, unexpected results of these applications emerged. Firstly, the online database of FAAPRED can only receive 25 sequences each time, which is not applicable for genome data. Secondly, Fungal RV is suitable for prediction for some medically important yeasts and *Aspergillus* strains (Chaudhuri *et al.* 2011), but results were inappropriate for dermatophytes: e.g. 5 probable adhesins were yielded for *T. rubrum* CBS 118892 and 25 for *T. rubrum* CBS 139224. Thirdly, GPI-anchor Predictor has a similar problem as Fungal RV, with unstable results for dermatophytes. For these reasons three software products were selected for our prediction, i.e. SIGNALP, GPI-modification and TMHMM Server, which produced consistent results among nine genomes. Putative adhesins were chosen with the following parameters: SIGNALP 4.0 positive; TMHMM 2.0 < 1 helices and number of AA to exclude as 45 from N-terminus and 35 for C-terminus; BIG-PI positive.

Table S4 lists the probable adhesins for nine dermatophytes. *Nannizzia gypsea* carried only five adhesins, while *Microsporum canis* had 17 adhesins. In *Trichophyton*, the number varied from 20 to 26, most being hypothetical proteins but some were known adhesins and GPI-anchor proteins, e.g. EGE03127.1 of T. *equinum* and EEQ28337.1 of *M. canis*. These sequences are ecm33, a gene encoding adhesins in *Saccharomyces cerevisiae*, *Candida albicans* and *Aspergillus fumigatus*. EFQ97364.1 and EFQ97072.1 of *N. gypsea* are gel4 and gel12, important genes facilitating adherence of *A. fumigatus* (Free 2013). Among the 21 genes predicted as adhesins for *T. rubrum*, 17 sequences are very similar to those of *T. violaceum*, which implies that *T. rubrum* has four specific adhesins and *T. violaceum* has eight.

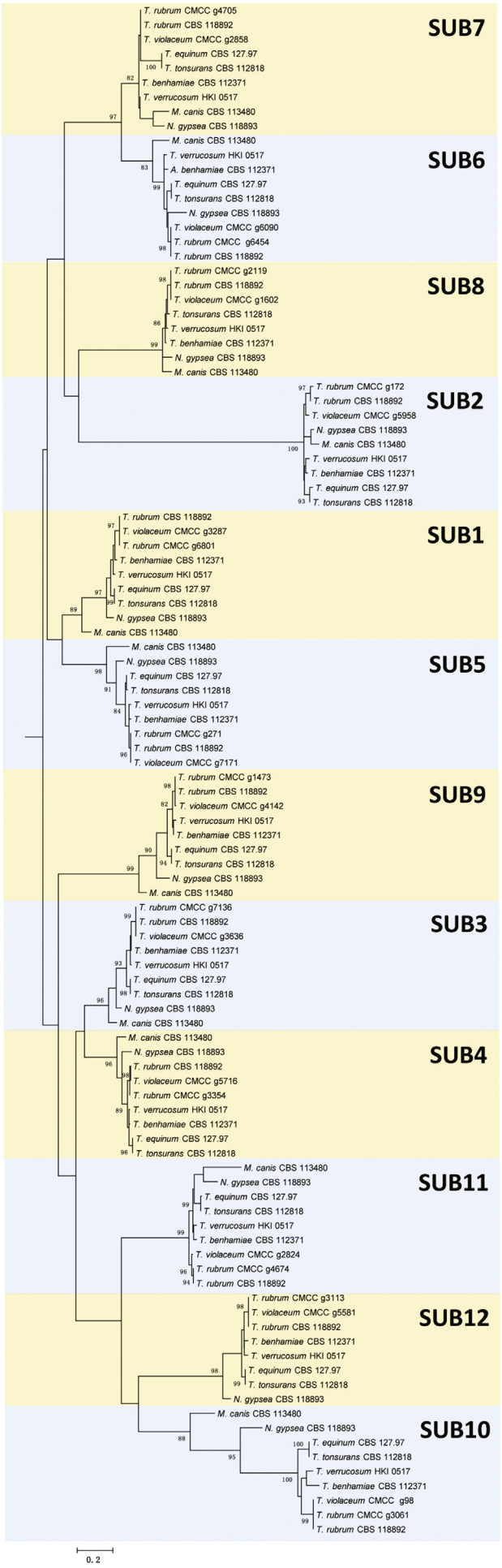

Secreted proteases

Three kinds of endoproteases belonging to three families were analyzed in the nine dermatophytes under study, including metalloproteases (M36 family), deuterolysins (M35 family) and subtilisins (S8A family) (Li & Zhang 2014, Tran *et al.* 2016, Martinez *et al.* 2012). Five duplicated genes belonging to metalloprotease and five genes belonging to deuterolysin persist in the genomes. M35 family members have high sequence similarity with neutral protease 2 and clustered in the M35-A clade (Li & Zhang 2014), which is specific for *Arthrodermataceae*. The different protease families showed comparable patterns of similarity, with four clusters: (1) *T. tonsurans* and *T. equinum*, (2) *T. verrucosum* and *T. benhamiae*, (3) *T. rubrum* and *T. violaceum*, and (4) *M. canis* and *N. gypsea*. This corresponds to known phylogenetic distances where sequences of *T. rubrum* and *T. violaceum* are highly similar, rather closely related to other *T. tonsurans/ equinum*, while *Microsporum* and *Nannizzia* are remote (Rezaei-Matehkolaei *et al.* 2014; de Hoog *et al.* 2017). Previous studies suggested that exoprotease genes have expanded independently (Li & Zhang 2014). The non-rooted trees of M35 and M36 showed similar topology suggesting that the families evolve with comparable speed, and the clustering was largely consistent with known phylogenetic relationships among the studied fungi. For this reason, we denominated the M35 genes as NP-2a to NP-2e in the order of MEP1–5 genes, for easy comparison (Fig. 6).

A total of 106 sequences were identified in the S8A family, comprising 12 sequences types which designated as Sub1 to Sub12 in the tree, except for Sub12 which was lost in *M. canis* and Sub8 lost in *T. equinum* (Fig. 7, Table S5). Two other subtilisin-like proteases (A7D00_1654 and A7D00_4929) which also contained an S8 domain were found in the genome of *T. rubrum* CBS 139224, but they had low identity with the classical S8A family. No similar sequences were found in *T. violaceum* CBS 141829. The S8A family showed much more diversity and a correspondence with phylogenetic relations was noted, as Sub7 is much closer to Sub6 and Sub8 and Sub2 may have evolved from this ancestor. The sequences could be grouped in two main clusters, with the upper one including Sub7, Sub6, Sub8, Sub2, Sub1 and Sub5, while the lower contained Sub9, Sub3, Sub4, Sub11, Sub12 and Sub10. Comparing the dendrogram of dermatophyte proteinase trees to the ribosomal tree, a similar topology became apparent. Members within the above families are listed in Table S5.

In addition to endoproteases, exoproteases play an important role in the degradation of hard keratin; these include dipeptidyl peptidase IV (DPPIV), dipeptidyl peptidase V (DPPV), leucine aminopeptidases (LAPs), carboxypeptidase A (MCPA), carboxypeptidase B (MCPB), carboxypeptidase S1 homolog A (SCPA), and carboxypeptidase S1 homolog B (SCPB) (Monod 2008; Tran *et al.* 2016). SED1and SED2 are genes belonging to tripeptidyl-peptidases which degrade proteins at acidic pH and are known to be involved in virulence of *Aspergillus fumigatus* (Reichard *et al.* 2006). Genes A7D00_5713 and A7C99_545 have high identity (over 90 %) with SED2 of *A. fumigatus*, but for SED1 no homologs were found. All proteinases annotated were displayed in Table S6.

Fig. 7. Non-rooted Maximum likelihood trees of dermatophyte secreted proteases (S8A families) constructed with MEGA v. 6.0 with 500 bootstrap replications.

Secondary metabolism

Table S7 lists the results of secondary metabolism of *T. rubrum* CBS 139224 and *T. violaceum* CBS 141829. Totally nine metabolite clusters are present in both fungi, seven of which are conserved. Additionally, there is an ochratoxin A biosynthetic gene cluster specific for *T. rubrum* with high identity (66 %) to *Penicillium nordicum* (AY557343), which is absent in *T. violaceum*. Two specific clusters, i.e. patulin biosynthetic and fusaridione A biosynthetic gene cluster, seem to be present in *T. violaceum*, but the results are uncertain, with only 13 % and 12 % identity with reference sequences.

DISCUSSION

The family *Arthrodermataceae* has recently been revised on the basis of molecular phylogeny (de Hoog *et al.* 2017). Ancestral, mostly geophilic dermatophytes with thick-walled macroconidia were placed in *Arthroderma*, while *Trichophyton* was restricted to a clade which covers all anthropophiles in addition to some zoophilic species. Ribosomal genes ITS and partial LSU are sequenced as standard, but in order to obtain better resolution, *TUB2*, *RP 60S L1*, *TEF*3 were included in addition. Surprisingly and in conflict with most other groups of filamentous fungi, best resolution (highest number of supported clades) was obtained with ITS (Table 3). Monophyly was confirmed for the currently distinguished seven genera (de Hoog *et al.* 2017). All seven genera were represented as clades by ITS with BS > 80 %, and for *Nannizzia* ITS was even the only marker with sufficient support. Average performance was achieved with *TUB2* and *RP 60S L1,* while LSU and *TEF3* had very poor performance.

The final phylogenetic overview of *Arthrodermataceae* was reconstructed on the basis of ITS is used as barcoding marker, with *Guarromyces ceretanicus* as outgroup in the tree constructed with Maximum likelihood using RAxML v. 8.0.0 under GTRCAT model and 1000 bootstrap replications (Fig. 2). The obtained phylogeny has a topology which in main traits confirmed early phylogenies published by Gräser *et al.* (2000), with seven bootstrap-supported clades now recognized as genera (de Hoog *et al.* 2017). Since *Homo sapiens* is the phylogenetically most recent mammal host of dermatophytes, the strictly anthropophilic species should appear in derived position in the tree. *Arthroderma*, comprising prevalently geophilic species, is found as an ancestral group. *Arthroderma* contains 21 currently accepted, mostly well-resolved species associated with burrows and furs of wild animals. Species occurring on domesticated animals are found near the anthropophiles (Fig. 2). Accordingly, the tree shows an evolutionary trend of increasing association with mammal hosts. We may assume that this reflects a true phylogenetic history and therefore it can be expected that the tree is robust, providing stable nomenclature.

While *Arthroderma* species are easily distinguished with large barcoding gaps, and frequently produce elaborate gymnothecial sexual states, the anthropophilic *Trichophyton* species are difficult to distinguish molecularly, and no sexual fruit bodies are known. Some species are phenotypically reduced, in culture just producing hyphal elements or chlamydospore-like structures. Significant adaptations are needed to colonize the hairless human skin, which may explain the loss of sexuality and reduced conidiation. Transmission takes place by skin flakes rather than by conidia or ascospores.

The close affinity of clinically different entities poses a diagnostic problem. The species *T. violaceum* is a highly specialized sibling of *T. rubrum*, having a predilection for the human scalp, while *T. rubrum* is found on skin and nails. As an alternative, it may be hypothesized that *T. violaceum* is just a phenotypically different strain of *T. rubrum* that has emerged because of differences in physiological stress exerted in different habitats. For correct affiliation of species and determination of species borderlines, understanding of virulence and adaptation are essential.

Epidemiological analyses suggested that the *Trichophyton rubrum* originated with humans in Africa and subsisted on this continent for a long time, often without causing significant disease (Gräser *et al.* 1999). This changed around the end of the nineteenth century when the fungus was transported on a worldwide scale via human travels and social activities. The fungus was also introduced to the Western world and became epidemic due to the preference of wearing closed leather shoes and sneakers as a part of modern life style (Gräser *et al.* 2000, 2007; Dismukes *et al.* 2003). In contrast, its close relative *T. violaceum* has remained in some endemic pockets in Africa and Asia as an agent of tinea capitis (Zhan *et al.* 2015) and was brought to Europe mainly by scattered, recent immigration events; it shows no tendency to epidemic expansion (Nenoff *et al.* 2014). In contrast to the globally widespread *T. rubrum*, *T. violaceum* as an endemic fungus is restricted to semiarid climate zones of the Mediterranean, Northern Africa, Iran and Northwestern and Southern China (Ayanbimpe *et al.* 2008; Patel & Schwartz 2011; Zhan *et al.* 2015). Using microsatellites, Ohst *et al.* (2004) demonstrated that *T. violaceum* showed more variation, while *T. rubrum* was nearly monomorphic suggesting a founder effect after adaptation to a new ecological niche. As a zoophilic species, *Trichophyton benhamiae* causes inflammatory disease when transmitted to humans (Drouot *et al.* 2009), while obligatorily anthropophilic species such as *T. rubrum* show low inflammation. In addition, the zoophile *T. benhamiae* is sexually competent. Li *et al.* (2010) reported that common features of the *MAT* locus are shared among five common dermatophytes (*N. gypsea*, *M. canis*, *T. equinum*, *T. rubrum* and *T. tonsurans*). Evolution of the *MAT* locus apparently is not synchronous with that of ecologically relevant parameters, and occasional successful mating between classical species can be observed (Kawasaki 2011). Our data in nine dermatophytes are consistent with these reports showing that the *MAT* locus is shared among species. Both *T. rubrum* and *T. violaceum* presented as *MAT1-1* mating type in our study, suggesting drift of unbalanced mating types leads to loss of mating in anthropophilic species (Gräser *et al.* 2008).

Genome sequencing has become one of the conventional means to study the biology and ecological abilities of microbes. Pacific Biosciences developed the single-molecule real-time sequencing technique (SMRT) which enables long reads (up to 23 000 bp) and has high efficiency of 1 080 Mb each run. However, the raw data generated from the PacBio RS platform is inherently error-prone, with up to 17.9 % errors having been reported (Chin *et al.* 2011). Most of these concerns *indel* events caused by incorporation events, or intervals that are too short to be reliably detected (Eid *et al.* 2009). The PacBio platform has been widely used in viruses, bacteria and small genome size organisms, but thus far rarely for fungi of medical interest. In our study we applied two genome sequencing platforms to obtain maximum genome quality, i.e. an Illumina platform with high

accuracy, as well as a PACBIO RS platform which allows long reads. Considering the high consistence of the compared species, and given the high cost of PacBio, there is no need for additional SMRT sequencing of *T. violaceum*. *Trichophyton rubrum* CBS 139224 yielded sequences with less scaffolds and with an N % as low as 0.055 %, which is much better than the presently available genome of *T. rubrum* CBS 118892. In addition we reconstructed the complete mitochondrial genome of *T. rubrum* CBS 139224 and *T. violaceum* CBS 141829, which showed high similarity to the previous report on this species (Wu *et al.* 2009).

The oriental strain *T. rubrum* CBS 139224 had a genome size of 22.3 Mb, CBS 118892 was published to be 22.5 Mb, while *T. violaceum* (CBS 141829) had 23.4 Mb. The genomes were compared with each other and with seven dermatophyte species available in the public domain. Four *Trichophyton* species ranged in size from 22.6 to 24.1 Mb. Draft genomes of dermatophytes show very high degrees of conservation, both at nucleotide and at amino acid levels (Martinez *et al.* 2012).

Most genomes of Eukaryotes, including fungi contain significant amounts of repetitive DNA, which usually occur in multiple copies and are with or without coding domains. In *Candida albican*s, major repeat sequences (MRS) have been identified in all but one chromosome (Lephart & Magee 2006). The *Aspergillus fumigatus* genome harbors rich duplication events, the majority clustering in 13 chromosomal islands, which are related to pathogenesis of clinical strains (Fedorova *et al.* 2008). Copy numbers and location may differ between populations and are stably inherited; the elements have widely been used in epidemiological profiling. Contrary to these fungi, dermatophytes show an extraordinarily high coherence at nucleotide and gene level, with very few repeat elements in the genome. These data indicate that dermatophytes are consistent pathogens with a short divergence time; very few genetic events occurred in the evolutionary history of dermatophytes.

Secreted proteases are key virulence factors for dermatophytes. Two types of endo-proteases are prevalent in dermatophytes, i.e. subtilisins belonging to the S8A family, and metalloproteinases which comprise two different subfamilies, the deuterolysins (M35) and the fungalysins (M36) (Monod 2008; Li & Zhang 2014). These proteases share high consistence among members of the same family, but have low degrees of identity among different families (Li & Zhang 2014). The protease families M35 (deuterolysins) and M36 (fungalysin) are among the most important metalloproteinases, in which zinc is an essential metal ion required for catalytic activity. These genes are found in numerous pathogenic fungi, but show expansion in *Arthrodermataceae* (dermatophytes) and *Onygenaceae* (the family containing *Coccidioides*; Li & Zhang 2014). Members of the M35 and M36 families seem to be highly conserved among dermatophytes with signatures that are specific for *Arthrodermataceae* and have low identity with other *Onygenales* (Li & Zhang 2014). In our study, M35 and M36 have the same five copies in all nine dermatophytes. As suggested by Li & Zhang (2014), M35 duplicated and M36 was lost in *Coccidioides* compared to dermatophytes, probably due to different life styles of these fungi as systemic and cutaneous pathogens, respectively.

Thus far twelve subtilisin-encoding genes within the S8A family have been reported (Martinez *et al.* 2012) and in our study, they were successfully annotated in nine genomes (see Methods), with the exception of *M. canis* (Sub12 lost) and *T. equinum* (Sub8 lost), which both have their natural niche in animal fur (Martinez *et al.* 2012). Phylogenetically, *T. rubrum* (human skin) is close to *T. violaceum* (human scalp), *T. equinum* (horse) is close to *T. tonsurans* (human skin), and *T. verrucosum* (cattle) close to *T. benhamiae* (guinea pigs), while all these species are remote from *Microsporum canis* (dog) and *Nannizzia gypsea* (soil). These data matched well with known phylogenetic relationships (de Hoog *et al.* 2017). A high degree of similarity was found between *T. rubrum* and *T. violaceum*; no unambiguous protease difference explaining the clinical difference between the two species was found, suggesting that the divergence between the entities concerns a very recent evolutionary event.

The two ecological niches of skin and scalp differ in the constitution of keratins, lipids, and immunity (Bolognia *et al.* 2008; Wolff *et al.* 2008). K1/K10 and K5/K14 are the most common keratins expressed in skin (designated as 'soft keratin'), while Hakb1-8 and Haka1-6 are only expressed in hair-follicles ('hard keratin'; Schweizer *et al.* 2007). Distribution of lipids and melanocytes are also quite different between skin and scalp. Our genome data indicate that the two species possess a high molecular conservation with 99.9 % identity at the amino acid level. Only 17 species-specific genes were discovered by protein-domain analysis. However, the genome of *T. violaceum* (23.4 Mb) is larger than that of *T. rubrum* (22.3–22.5 Mb), with more unigenes (7 415 *vs.*7 170). This is consistent with the recent global expansion and adaptation in *T. rubrum,* assuming that the species reduced superfluous antigens while adapting to superficial invasion of the skin.

Adherence to host tissue is a prerequisite for microorganisms for invasion and infection (de Groot *et al.* 2013). Fungal adhesins are cell wall proteins with a highly conserved signal peptide at the N-terminus and a GPI-anchor at the C-terminus. This enables prediction of putative adhesins by bioinformatics. At least three families are known: anagglutinin-like sequences (ALS) family, a hyphal wall protein (HWP) family, and an IFF/HYP family with over 20 genes (Mayer *et al.* 2013). RodA, CalA and CspA enhance adherence to bronchial epithelial cells in *Aspergillus* (Jahn *et al.* 2000; Levdansky *et al.* 2010), but as yet no adhesin genes have been reported for dermatophytes because of insufficiency of genetic tools. FUNGALRV (Chaudhuri *et al.* 2011) and FAAPRED have been applied (Chaudhuri *et al.* 2011; de Groot *et al.* 2013; Teixeira *et al.* 2014), but in our study SIGNALP, GPI-modification and the TMHMM server proved to be more successful. We found about 20 adhesins in each dermatophyte studied here except *N. gypsea*, which matches with its life style as a geophilic fungus. Some genes even align well with known adhesins from non-dermatophyte species. *Trichophyton rubrum* and *T. violaceum* possess 17 common adhesins, four being specific for the former and 8 for the latter. It seems plausible that the clinical difference between these species might be at least partly ascribed to these adhesins.

An alternative hypothesis for the clinical divergence of *T. rubrum/ T. violaceum* might be their interpretation as a single species which shows epigenetic change when growing on either the scalp or on naked skin. Possibly some pathways such as the polyketide pathway are blocked with growth on the scalp, leading to reduced sporulation and growth and to formation of pigmented secondary metabolites seen in *T. violaceum* cultures, which can be restored by repeated transfer on artificial media; sporulation is vitamin B dependent (Gräser *et al.* 2000). Phenotypic segregates *T. soudanense*, *T. gourvilii* and *T. yaoundei* are as yet not reliably distinguishable molecularly from *T. violaceum* and might concern mutated forms or strains in stress response. Given the probably

haploid condition of these fungi, genomic polymorphism is relatively easy and might provide some advantages in natural selection. However, this hypothesis does not match with microsatellite (Gräser *et al.* 2007) and Maldi-tof (A. Packeu, pers. comm.) data, which suggest a recent divergence of clonal *T. rubrum* from a more variable African gene pool.

ACKNOWLEDGEMENTS

This research was supported by the National Natural Science Foundation of China (31600120), CAMS Innovation Fund for Medical Science (CAMS-I2M, 2016-I2M-3-021), the Ministry of Science and Technology Foundation special projects (2013FY113700), and Jiangsu provincial Special Program of Medical Science (BL20122012003). We acknowledge Ye Tao for library construction, NGS sequencing and data analysis work at Shanghai Biozeron Biotechnology Co. Sarah Abdallah Ahmed is thanked for providing the photoplate of *T. rubrum* and *T. violaceum* phenotypes.

APPENDIX A. SUPPLEMENTARY DATA

Supplementary data related to this article can be found at https://doi.org/10.1016/j.simyco.2018.02.004.

REFERENCES

Ates AN, Ozcan K, Ilkit MT (2008). Diagnostic value of morphological, physiological and biochemical tests in distinguishing *Trichophyton rubrum* from *Trichophyton mentagrophytes* complex. *Medical Mycology* **46**: 811–822.

Ayanbimpe GM, Taghir H, Diya A, *et al*. (2008). Tinea capitis among primary school children in some parts of central Nigeria. *Mycoses* **51**: 336–340.

Bankevich A, Nurk S, Antipov D, *et al*. (2012). SPAdes: a new genome assembly algorithm and its applications to single-cell sequencing. *Journal of Computational Biology* **19**: 455–477.

Bao W, Kojima KK, Kohany O (2015). Repbase Update, a database of repetitive elements in eukaryotic genomes. *Mobile DNA* **6**: 11.

Bolognia JL, Jorizzo JL, Rapinl RP (2008). *Dermatology*, 2nd ed. Elsevier, London, UK.

Brankovics B, Zhang H, van Diepeningen AD, *et al*. (2016). GRAbB: Selective Assembly of Genomic Regions, a new niche for genomic research. *PLoS Computational Biology* **12** e1004753.

Burmester A, Shelest E, Glöckner G, *et al*. (2011). Comparative and functional genomics provide insights into the pathogenicity of dermatophytic fungi. *Genome Biology* **12**: R7.

Chaudhuri R, Ansari FA, Raghunandanan MV, *et al*. (2011). FungalRV: adhesin prediction and immunoinformatics portal for human fungal pathogens. *BMC Genomics* **12**: 192.

Chibana H, Oka N, Nakayama H, *et al*. (2005). Sequence finishing and gene mapping for *Candida albicans* chromosome 7 and syntenic analysis against the *Saccharomyces cerevisiae* gene. *Genetics* **170**: 1525–1537.

Chin CS, Sorenson J, Harris JB, *et al*. (2011). The origin of the Haitian cholera outbreak strain. *The New England Journal of Medicine* **364**: 33–42.

de Groot PWJ, Bader O, de Boer AD, *et al*. (2013). Adhesins in human fungal pathogens: glue with plenty of stick. *Eukaryotic Cell* **12**: 470–481.

de Hoog GS, Dukik K, Monod M, *et al*. (2017). Toward a novel multilocus phylogenetic taxonomy for the dermatophytes. *Mycopathologia* **182**: 5–31.

Dismukes WG, Peter G, *et al*. (2003). *Clinical Mycology*. Oxford University Press.

Drouot S, Mignon B, Fratti M, *et al*. (2009). Pets as the main source of two zoonotic species of the *Trichophyton mentagrophytes* complex in Switzerland, *Arthroderma vanbreuseghemii* and *Arthroderma benhamiae*. *Veterinary Dermatology* **20**: 13–18.

Eid J, Fehr A, Gray J, *et al*. (2009). Real-time DNA sequencing from single polymerase molecules. *Science* **323**: 133–138.

Elsik CG, Mackey AJ, Reese JT, *et al*. (2007). Creating a honey bee consensus gene set. *Genome Biology* **8**: R13.

Farina C, Fazii P, Imberti G, *et al*. (2015). *Trichophyton violaceum* and *T. soudanese*: re-emerging pathogens in Italy, 2005-2013. *New Microbiologica* **38**: 409–415.

Fedorova ND, Khaldi N, Joardar VS, *et al*. (2008). Genomic islands in the pathogenic filamentous fungus *Aspergillus fumigatus*. *PLoS Genetics* **4** e1000046.

Free SJ (2013). Fungal cell wall organization and biosynthesis. *Advances in Genetics* **81**: 33–82.

Gräser Y, Kühnisch J, Presber W (1999). Molecular markers reveal exclusively clonal reproduction in *Trichophyton rubrum*. *Journal of Clinical Microbiology* **37**: 3713–3717.

Gräser Y, Kuijpers AF, Presber W, *et al*. (2000). Molecular taxonomy of the *Trichophyton rubrum* complex. *Journal of Clinical Microbiology* **38**: 3329–3336.

Gräser Y, Fröhlich J, Presber W, *et al*. (2007). Microsatellite markers reveal geographic population differentiation in *Trichophyton rubrum*. *Journal of Medical Microbiology* **56**: 1058–1065.

Gräser Y, Scott J, Summerbell R (2008). The new species concept in dermatophytes-a polyphasic approach. *Mycopathologia* **166**: 239–256.

Havlickova B, Czaika VA, Friedrich M (2008). Epidemiological trends in skin mycoses worldwide. *Mycoses* **51**(Suppl 4): 2–15.

Jahn B, Boukhallouk F, Lotz J, *et al*. (2000). Interaction of human phagocytes with pigmentless *Aspergillus* conidia. *Infection and Immunity* **68**: 3736–3739.

Katoh K, Asimenos G, Toh H (2009). Multiple alignment of DNA sequences with MAFFT. *Methods in Molecular Biology* **537**: 39–64.

Kawasaki M (2011). Verification of a taxonomy of dermatophytes based on mating results and phylogenetic analyses. *Medical Mycology Journal* **52**: 291–295.

Kim MS, Kim JK, Lee MW, *et al*. (2015). Epidemiology of deep cutaneous fungal infections in Korea (2006–2010). *Journal of Dermatology* **42**: 962–966.

Koren S, Schatz MC, Walenz BP, *et al*. (2012). Hybrid error correction and *de novo* assembly of single-molecule sequencing reads. *Nature Biotechnology* **30**: 693–700.

Lephart PR, Magee PT (2006). Effect of the major repeat sequence on mitotic recombination in *Candida albicans*. *Genetics* **174**: 1737–1744.

Levdansky E, Kashi O, Sharon H, *et al*. (2010). The *Aspergillus fumigatus* cspA gene encoding a repeat-rich cell wall protein is important for normal conidial cell wall architecture and interaction with host cells. *Eukaryotic Cell* **9**: 1403–1415.

Li J, Zhang KQ (2014). Independent expansion of zinc in metalloproteinases in *Onygenales* fungi may be associated with their pathogenicity. *PLoS One* **9**: e90225.

Li W, Metin B, White TC, *et al*. (2010). Organization and evolutionary trajectory of the mating type (*MAT*) locus in dermatophyte and dimorphic fungal pathogens. *Eukaryotic Cell* **9**: 46–58.

Marchler-Bauer A, Bryant SH (2004). CD-Search: protein domain annotations on the fly. *Nucleic Acids Research* **32**: 327–331.

Martinez DA, Oliver BG, Gräser Y, *et al*. (2012). Comparative genome analysis of *Trichophyton rubrum* and related dermatophytes reveals candidate genes involved in infection. *MBIO* **3**: e00259–12.

Mayer FL, Wilson D, Hube B (2013). *Candida albicans* pathogenicity mechanisms. *Virulence* **4**: 119–128.

Mirhendi H, Makimura K, de Hoog GS, *et al*. (2015). Translation elongation factor 1-gene as a potential taxonomic and identification marker in dermatophytes. *Medical Mycology* **53**: 215–224.

Mitchell A, Chang HY, Daugherty L, *et al*. (2015). The InterPro protein families databases: the classification resources after 15 years. *Nucleic Acids Research* **43**: 213–221.

Monod M (2008). Secreted proteases from dermatophytes. *Mycopathologia* **166**: 285–294.

Nenoff P, Krüger C, Ginter-Hanselmayer G, *et al*. (2014). Mycology-an update. Part 1: Dermatomycoses: Causative agents, epidemiology and pathogenesis. *Journal der Deutschen Dermatologischen Gesellschaft* **12**: 188–210.

Nierman WC, Pain A, Anderson MJ, *et al*. (2005). Genomic sequence of the pathogenic and allergenic filamentous fungus *Aspergillus fumigatus*. *Nature* **438**: 1151–1156.

Ohst T, de Hoog GS, Presber W, *et al*. (2004). Origins of microsatellite diversity in the *Trichophyton rubrum-T. violaceum* clade (dermatophytes). *Journal of Clinical Microbiology* **42**: 4444–4448.

Patel GA, Schwartz RA (2011). Tinea capitis: still an unsolved problem? *Mycoses* **54**: 183–188.

Pavesi A, Conterio F, Bolchi A, *et al*. (1994). Indentification of new eukaryotic tRNA genes in genomic DNA databases by a multistep weight matrix

analysis of transcriptional control regions. *Nucleic Acids Research* **22**: 1247–1256.

Ramana J, Gupta D (2010). FaaPred: a SVM-based prediction method for fungal adhesins and adhesin-like proteins. *PLoS One* **5** e9695.

Reichard U, Léchenne B, Asif AR, *et al*. (2006). Sedolisins, a new class of secreted proteases from *Aspergillus fumigatus* with endoprotease or tripeptidyl-peptidase activity at acidic pHs. *Applied and Environmental Microbiology* **72**: 1739–1748.

Rezaei-Matehkolaei A, Mirhendi H, Makimura K, *et al*. (2014). Nucleotide sequence analysis of beta tubulin gene in a wide range of dermatophytes. *Medical Mycology* **52**: 674–688.

Schweizer J, Langbein L, Rogers MA, *et al*. (2007). Hair follicle-specific keratins and their diseases. *Experimental Cell Research* **313**: 2010–2020.

Stanke M, Morgenstern B (2015). Augustus: a web server for gene prediction in eukaryotes that allows user-defined constraints. *Nucleic Acids Research* **33**: W465–W467.

Stielow JB, Lévesque CA, Seifert KA, *et al*. (2015). One fungus, which genes? Development and assessment of universal primers for potential secondary fungal DNA barcodes. *Persoonia* **35**: 242–263.

Teixeira MM, de Almeida LG, Kubitschek-Barreira P, *et al*. (2014). Comparative genomics of the major fungal agents of human and animal sporotrichosis: *Sporothrix schenckii* and *Sporothrix brasiliensis*. *BMC Genomics* **5**: 943.

Ter-Hovhannisyan V, Lomsadze A, Chernoff YO, *et al*. (2008). Gene prediction in novel fungal genomes using an *ab initio* algorithm with unsupervised training. *Genome Research* **18**: 1979–1990.

Tran VD, De Coi N, Feuermann M, *et al*. (2016). RNA sequencing-based genome reannotation of the dermatophyte *Arthroderma benhamiae* and characterization of its secretome and whole gene expression profile during infection. *mSystems* **2** e00036-16.

Vu TD, Eberhardt U, Szöke S, *et al*. (2012). A laboratory information management system for DNA barcoding workflows. *Integrative Biology* **4**: 744–755.

Weber T, Blin K, Duddela S, *et al*. (2015). antiSmash 3.0-a comprehensive resource for the genome mining of biosynthetic gene clusters. *Nucleic Acids Res*. **43**: 237–243.

Wolff K, Goldsmith L, Katz S, *et al*. (2008). *Fitzpatrick's dermatology in general medicine*, 7th edn. McGraw-Hill Companies, Inc., USA.

Wu Y, Yang J, Yang F, *et al*. (2009). Recent dermatophyte divergence revealed by comparative and phylogenetic analysis of mitochondrial genomes. *BMC Genomics* **10**: 238.

Zhan P, Li D, Wang C, *et al*. (2015). Epidemiological changes in tinea capitis over the sixty years of economic growth in China. *Medical Mycology* **53**: 691–698.